



# Photogrammetry and LiDAR from UAS in steep terrain

Recommendations for acquiring data in steep terrain: flight  
planning and data processing

STATENS VEGVESENS RAPPORTER

Nr. 991



## Tittel

Photogrammetry and LiDAR from UAS in steep terrain

## Undertittel

Recommendations for acquiring data in steep terrain: flight planning and data processing

## Forfatter

Bastien Dupuy (editor) with co-authors from SINTEF, NGI and NPRA (see page 3)

## Avdeling

Fagressurs Drift og vedlikehold

## Seksjon

Geofag Drift og vedlikehold

## Prosjektnummer

C15115

## Rapportnummer

991

## Prosjektleder

Tore Humstad

## Godkjent av

Halgeir Dahle

## Emneord

UAV, UAS, fjernanalyse, snøoverflate, snødybde, snøskredvarsling

## Sammendrag

Denne rapporten beskriver prosedyrer og anbefalinger for innhenting av fjernmålingsdata over snøoverflater. Den inkluderer planlegging av undersøkelser og databehandlingsrutiner for høyoppløselig terrengkartlegging ved bruk av optiske kameraer og LiDAR-skanningsmetoder, både ved bruk av kommersielle og åpen kildekode-verktøy.

## Title

Photogrammetry and LiDAR from UAS in steep terrain

## Subtitle

Recommendations for acquiring data in steep terrain: flight planning and data processing

## Author

Bastien Dupuy (editor) with co-authors from SINTEF, NGI and NPRA (see page 3)

## Department

O&M Planning and Engineering Services

## Section

O&M Geomechanics

## Project number

C15115

## Report number

991

## Project manager

Tore Humstad

## Approved by

Halgeir Dahle

## Key words

UAV, UAS, remote sensing, snow surface, snow height, avalanche forecasting

## Summary

This report describes procedures and recommendations for acquisition of remote sensing data over snow surfaces. It includes survey planning and data processing routines for high resolution terrain mapping using optical cameras and LiDAR scanning methods, both using commercial and open-source tools.



SINTEF

+

# Report

## GEOSFAIR (Geohazard Survey from Air) deliverable D2.1

Recommendations for acquiring photogrammetry and LiDAR data in steep terrain: flight planning and data processing

### Authors:

Andrew Tobiesen, Halgeir Dahle, Bastien Dupuy, Sean Salazar, Regula Frauenfelder, Arnt Grøver, Tore Humstad, Emil Solbakken, Aslak Einbu

### Report No:

2024:00844 - Unrestricted

### Clients and partners:

The research council of Norway, NPRA, NGI



SINTEF

SINTEF Industry  
Postal address:  
Postboks 4763 Torgarden  
7465 Trondheim

Switchboard: +47 40005100  
info@sintef.no

Enterprise /VAT No:  
NO 919 303 808 MVA

# Report

## GEOSFAIR (Geohazard Survey from Air) deliverable D2.1

Recommendations for acquiring photogrammetry and LiDAR data in steep terrain: flight planning and data processing

### KEYWORDS

UAV, remote sensing,  
snow surface, snow  
height, avalanche  
forecasting

### VERSION

5

### DATE

2024-07-05

### AUTHOR(S)

Andrew Tobiesen, Halgeir Dahle, Bastien Dupuy, Sean Salazar, Regula Frauenfelder, Arnt Grøver, Tore Humstad, Emil Solbakken, Aslak Einbu

### CLIENTS AND PARTNERS

The research council of Norway, NPRA, NGI

### CLIENT'S REFERENCE

321035/080

### PROJECT NO.

102025034

### NO. OF PAGES

42

### SUMMARY

This report describes procedures and recommendations for acquisition of remote sensing data over snow surfaces. It includes survey planning and data processing routines for high resolution terrain mapping using optical cameras and LiDAR scanning methods, both using commercial and open-source tools.

### PREPARED BY

Bastien Dupuy

### SIGNATURE

Bastien Dupuy

### CHECKED BY

Madeline Lee

### SIGNATURE

Madeline Lee

### APPROVED BY

Peder Eliasson

### SIGNATURE

Peder Eliasson

COMPANY WITH  
MANAGEMENT SYSTEM  
CERTIFIED BY DNV  
ISO 9001 • ISO 14001  
ISO 45001

### REPORT NO.

2024:00844

### ISBN

978-82-14-07057-6

### CLASSIFICATION

Unrestricted

### CLASSIFICATION THIS PAGE

Unrestricted

# Document history

VERSION	DATE	VERSION DESCRIPTION
1	2022-12-09	Initial versions on photogrammetry open-source and commercial tools and LiDAR commercial tools by Andrew Tobiesen, Halgeir Dahle, Sean Salazar
2	2024-01-11	Consistency updates, ready for proofreading (Bastien Dupuy)
3	2024-02-21	Clean version after proofreading, ready for final check (Bastien Dupuy)
4	2024-05-15	Version for internal QC
5	2024-07-05	Final version

# Table of contents

<b>1. Introduction .....</b>	<b>5</b>
<b>2. Recommendations for flight planning and autonomous data collection - photogrammetry .....</b>	<b>5</b>
2.1. General workflow and hardware .....	5
2.1.1. Conceptual workflow .....	6
2.1.2. UAV platforms and sensors .....	6
2.2. Mission planning .....	8
2.2.1. Importing accurate elevation data .....	11
Option1: Enhanced SRTM data for Scandinavia .....	11
Option 2: DEM data from the Norwegian mapping authority imported in Geotiff format...	11
2.2.2. Dry run simulation of survey .....	13
2.2.3. Terrain following optimization .....	14
2.2.4. Run the survey in simulation .....	14
2.2.5. Web application for flight execution .....	15
2.2.6. Degree of autonomy .....	16
2.3. Data/images recording .....	17
2.3.1. Georeferencing UAV images .....	17
2.3.2. PPK workflow for georeferencing .....	17
2.3.3. Creating batch data workflows .....	17
2.4. Data processing with open-source software .....	19
2.4.1. Photogrammetry workflow.....	19
2.4.2. Georeferencing, change detection and data interpretation .....	21
2.4.3. Validations at Tiller test site.....	23
2.5. Data processing with commercial software .....	27
2.5.1. Photogrammetry workflow.....	27
<b>3. Recommendations for flight planning and autonomous data collection – LiDAR .....</b>	<b>28</b>
3.1. General workflow and hardware .....	28
3.2. Flight planning.....	29
3.3. Data processing .....	31
3.3. Publishing of results .....	32
3.4. Data validation and interpretation .....	33
<b>4. Conclusions .....</b>	<b>33</b>

## APPENDICES

---

Klikk eller trykk her for å skrive inn tekst.

---

List of abbreviations:

API: application programming interface  
BVLOS: beyond visual line of sight  
DEM: digital elevation model  
DSM: digital surface model  
DTM: digital terrain model  
ESC: electronic speed controller  
GCP: ground control point  
GCS: ground control station  
GNSS: global navigation satellite system  
GPS: global positioning system  
GSD: ground sample distance  
KML: keyhole markup language  
LiDAR: light detection and ranging  
MTOW: maximum take-off weight  
NPRA: Norwegian public road administration  
PPK: post-processing kinematics  
PPP: precise point positioning  
RC: radio control  
RGB: red green blue  
RTK: real-time kinematics  
SfM: structure from motion  
SITL: software in the loop  
SRTM: shuttle radar topography mission  
UAV: uncrewed aerial vehicle  
UTM: universal transverse mercator  
WMS: web map service

# 1. Introduction

This report documents guidelines for recording UAV (Uncrewed Aerial Vehicle) remote sensing data for snow surface mapping. Extensive literature is available on the use of UAV using RGB (red, green, blue) cameras and a good overview is given by Bühler et al. (2016)<sup>1</sup> for photogrammetry of snow surfaces. On the other hand, laser sensors mounted on UAVs have been made possible only recently thanks to miniaturisation of LiDAR (Light Detection And Ranging) sensors as well as reduced weight, and only a few studies are available in the literature (e.g., Harder et al., 2020<sup>2</sup>, Cho et al., 2021<sup>3</sup>, Jacobs et al., 2021<sup>4</sup>, Koutantou et al., 2022<sup>5</sup>). In this report, we provide guidelines for:

- 1- Planning missions in steep mountainous terrain including BVLOS (Beyond Visual Line Of Sight) flights.
- 2- Recording data safely and efficiently with commercial and custom-made UAVs carrying camera and LiDAR payloads.
- 3- Processing the recorded data to derive high density point clouds and/or orthophotos and digital elevation models. We describe the use of commercial (photogrammetry and LiDAR) and open-source (photogrammetry) software solutions.

The report first describes recommendations for photogrammetry surveys using both commercial and open-source tools and provides examples of survey plans and recorded data. In the second part, the report describes guidelines for UAV LiDAR data acquisition for snow mapping and operational use in support of local snow avalanche forecasting.

## 2. Recommendations for flight planning and autonomous data collection - photogrammetry

### 2.1. General workflow and hardware

This chapter describes general procedures for creating surveys for photogrammetric mapping purposes. The procedures are also applicable to other survey types with different UAV payloads (LiDAR, multispectral camera, thermal camera etc.). The photogrammetry technique described herein is based generally on Structure-from-Motion (SfM) multi-view stereo algorithms, which provide high-resolution terrain models and georeferenced orthomosaics. The processing and interpretation workflow can be automated. The procedures were developed within the context of remote mapping of avalanche release areas (starting and runout zones), which present a potential hazard to infrastructure networks (e.g., roads).

---

<sup>1</sup> Bühler, Yves, Marc S. Adams, Ruedi Bösch, and Andreas Stoffel. "Mapping snow depth in alpine terrain with unmanned aerial systems (UASs): potential and limitations." *The Cryosphere* 10, no. 3 (2016): 1075-1088.

<sup>2</sup> Harder, Phillip, John W. Pomeroy, and Warren D. Helgason. "Improving sub-canopy snow depth mapping with unmanned aerial vehicles: lidar versus structure-from-motion techniques." *The Cryosphere* 14, no. 6 (2020): 1919-1935.

<sup>3</sup> Cho, Eunsang, Adam G. Hunsaker, Jennifer M. Jacobs, Michael Palace, Franklin B. Sullivan, and Elizabeth A. Burakowski. "Maximum entropy modeling to identify physical drivers of shallow snowpack heterogeneity using unpiloted aerial system (UAS) lidar." *Journal of Hydrology* 602 (2021): 126722.

<sup>4</sup> Jacobs, Jennifer M., Adam G. Hunsaker, Franklin B. Sullivan, Michael Palace, Elizabeth A. Burakowski, Christina Herrick, and Eunsang Cho. "Snow depth mapping with unpiloted aerial system lidar observations: a case study in Durham, New Hampshire, United States." *The Cryosphere* 15, no. 3 (2021): 1485-1500.

<sup>5</sup> Koutantou, Kalliopi, Giulia Mazzotti, Philip Brunner, Clare Webster, and Tobias Jonas. "Exploring snow distribution dynamics in steep forested slopes with UAV-borne LiDAR." *Cold Regions Science and Technology* 200 (2022): 103587.



### 2.1.1. Conceptual workflow

Figure 1 provides an overall workflow for the UAV surveys. Starting from pre-flight preparations, including mission planning which can be checked with flight simulation, the UAV survey is carried out together with automatic data recording. The data upload and data processing steps lead to the creation of results that can help in decision-making about further actions to be taken.

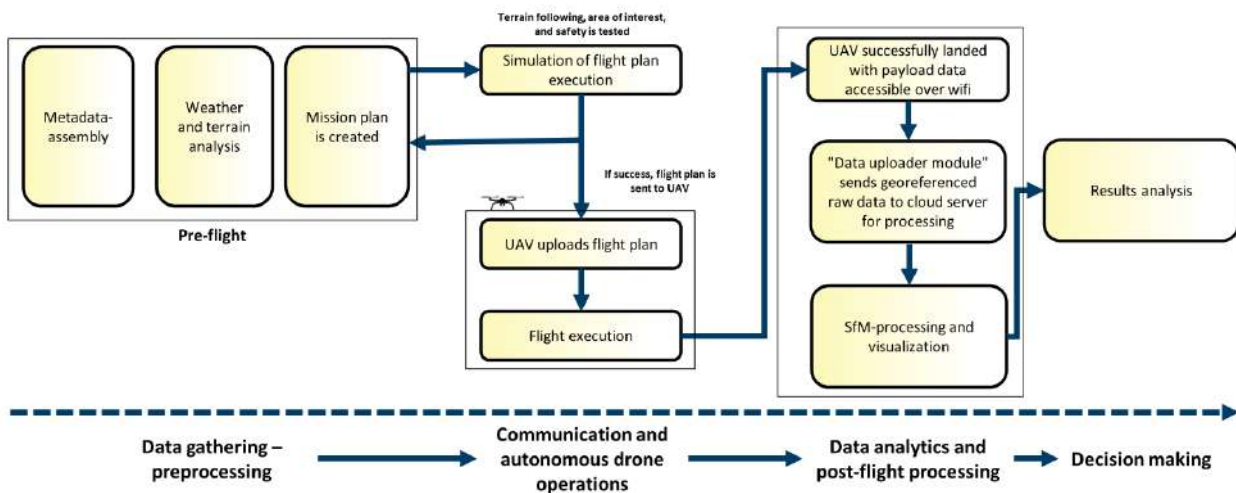


**Figure 1: Overall workflow describing pre-flight planning and simulation, flight execution and data recording, data processing and result analysis.**

### 2.1.2. UAV platforms and sensors

Various commercial off-the-shelf camera sensor options are available for UAV photogrammetry applications, using both multicopters and fixed wing aircraft systems, including e.g., DJI Matrice 300 RTK with Zenmuse P1, DJI Mavic 3 Enterprise RTK, etc. The general workflow for setting up flight planning and drone flight with data capture as well as post processing of data such as image georeferencing and further elevation model creation, is conceptually very similar both for custom and commercial off-the-shelf UAVs. With access to open API's and interface programming knowledge, it is possible to a large extent to automate the workflow using open-source platforms. Flight planning with commercial software is addressed in section 3 for LiDAR surveys. Differences between commercial and open-source software for photogrammetry data processing are highlighted in sections 2.4 and 2.5.

In this section, we describe the UAV survey workflow using SINTEF Industry's GeoDrones UAV platform "Prototype One" which has direct RC (Radio Control) communication using Mavlink communication protocol<sup>6</sup>. The aim has been to enable fully automated flights that are performed using a pre-calibrated camera, from start to finish, with no operator input or manual flight control (an operator may however abort a mission, or take control remotely, at any time). The flights are supervised from a custom developed application run on a ground control station (GCS) connected through telemetry. As with professional, survey-grade UAVs available on the market, the custom UAV system described herein relies on real-time kinematic (RTK) corrections to ensure accurate positioning data.

<sup>6</sup> <https://mavlink.io/en/>

A criterion for development has been to use clear communications protocols between different software platforms and access to the UAV payload. This makes development more "future proof", more flexible, and avoids potential lock-in technology. The data workflow and automation of results has mainly consisted of using open-source mathematical libraries in Python and C++ programming languages. The motivations for a tailored built vehicle are total control of both hardware and software, integration of existing software and clear access to APIs (application Programming Interfaces).

A camera payload is mounted on the custom UAV and produces image data geotagged with RTK-positioning. Available camera payloads are Sony α6000, Sony RX100 and multispectral Micasense Red-edge camera. In the following documentation, the testing has been conducted with the Sony α6000 24MP camera. The type of electronics is replaceable, follows an open hardware architecture and can be used as basis for further development. The UAV runs on Ardupilot<sup>7</sup>. The following details the GeoDrones "Prototype One" specifications:

**UAV performance:**

1. Flight time: 45-60 minutes
2. Max wind resistance: 14 m/s
3. Terrain following in all auto modes

**Camera payload:**

4. Camera resolution: 24 MP RGB (Sony α6000)
5. Ground sample distance (GSD): ~2.5 cm/px at 100 m altitude

**Other possible payload sensors:**

6. Multispectral camera
7. Thermal camera
8. LiDAR

**UAV technical specifications:**

9. Frame materials: carbon fiber
10. Maximum take-off weight (MTOW): 3.5 kg
11. Dry weight: 1.4 kg
12. Battery capacity: 22.2 V, 7-12 Ah (6S)
13. Size:
  - Wheelbase: 610 mm
  - Folding size: 285\*285\*175 mm
  - Unfolded size: 640\*640\*280 mm
14. Propellers: 15' folding propellers
15. Max recommended air speed: 20 m/s
16. Dual GPS (Global Positioning System) with RTK-GNNS (Global Navigation Satellite System)
17. Workflow: PPK (Post-Processed Kinematics), RTK, PPP (Precise Point Positioning)

**Redundancy and security:**

18. Separate current module to FC unit
19. Dual GPS blended signal
20. Running two autopilot cores in parallel

---

<sup>7</sup> <https://ardupilot.org/>

21. Two independent radio systems for control
22. Geofencing
23. Tested operational temperature in the interval of -20°C to +40°C

Note, there is no redundancy in motor propulsion as the aircraft is a quadcopter, with 4 motors. Due to the potential for a single point of failure, the propulsion system requires quality-tested motors and ESCs (Electronic Speed Controllers). Dual GPS ensures redundancy in navigation mode as long as GPS is available. If GPS falls out for a prolonged period, the UAV is at some point ordered to land. Figure 2 shows a picture of the UAV.



Figure 2. Example of the GeoDrones "Prototype One" platform.

## 2.2. Mission planning

A typical survey location will be determined based on assumed hazard zones and areas where it is necessary to assess conditions. Survey areas can be based on initial observations or modelled areas that are historically danger zones. The workflow described herein includes the capabilities to extend creation of missions with more advanced mission planning e.g., by adding statistical models and value-of-information (VOI) concepts for identifying survey location(s).

For testing the mission planning procedures, the SINTEF's UAV test site at Tiller, near Trondheim, Norway (Figure 3) has been extensively used. In addition, several simulations have been conducted in Storlidalen, Norway, which is characterized by large mountain surroundings and avalanche paths that enabled stress testing of the UAVs as well as the work procedures.



**Figure 3. Test site at Tiller, Trondheim.**

When the survey location has been identified, the survey grid must be created. Figure 4 shows an example of a surveyed area on the south-east side of Storhaugen in Storlidalen. Our general procedure is to use the Mission Planner software<sup>8</sup>, which is an open-source platform ground control station specifically created for the Ardupilot autopilot. UgCS mission planner<sup>9</sup> and QgroundControl<sup>10</sup> are other software that have been tested and used by SINTEF.

---

<sup>8</sup> <https://ardupilot.org/planner/>

<sup>9</sup> <https://www.ugcs.com/>

<sup>10</sup> <http://qgroundcontrol.com/>

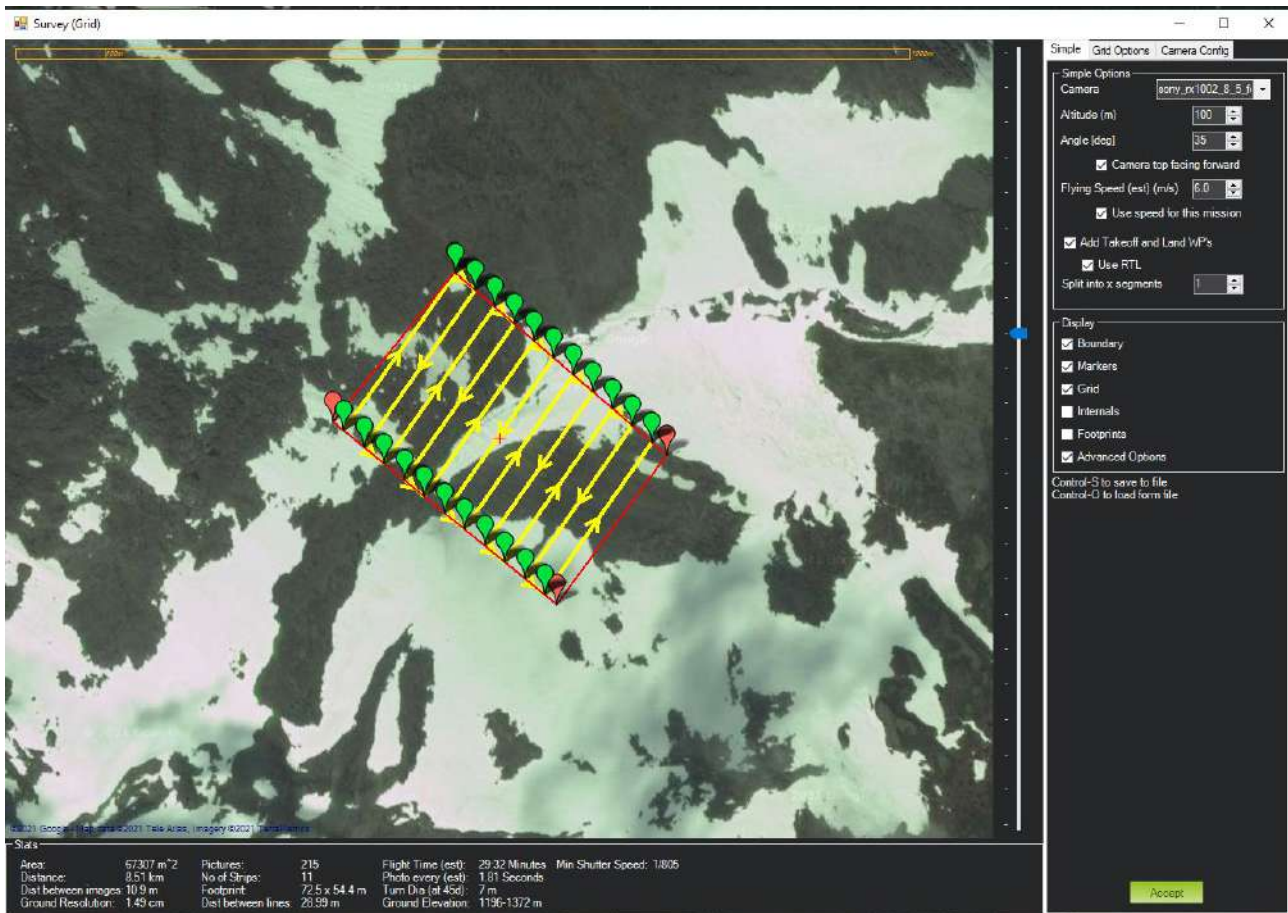


**Figure 4. Transects across an avalanche starting zone in Storlidalen (set up for simulation, using Mission Planner/SITL software)**

A procedure found for completing a mission on a mountain in a most energy efficient manner (for the UAV operation) requires one to create the survey in a way such that the highest point of the survey is completed first, thereby following gradually lower transects where each of the transects have similar altitude (i.e., following the terrain, see Figure 4). Figure 5 shows an example of the full flight path, including transport from landing and take-off spots, as well as the photogrammetry grid covering the potential avalanche starting zone on the southeast side of Storhaugen mountain. Note that these tests require BVLOS procedures due to long distance between survey area and take-off/landing locations, requiring a special operations permit in Norway. For this example, the survey has only been conducted in a simulated environment.

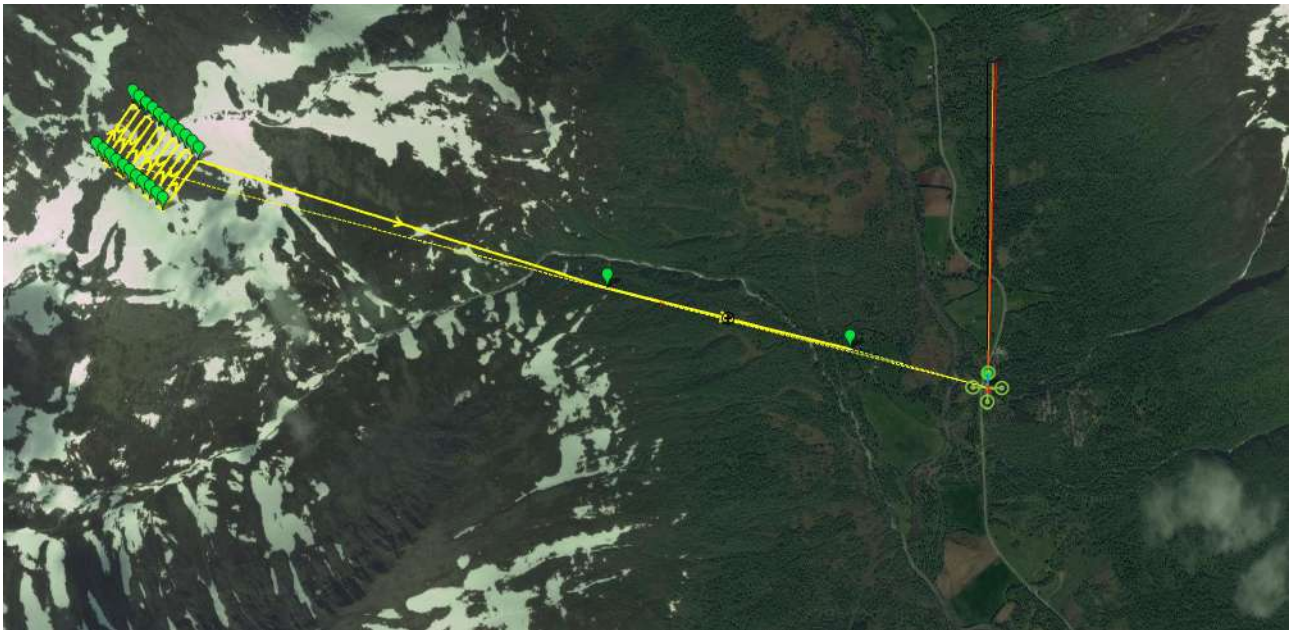


Figure 5. Flight path and survey from the main road to the "avalanche starting zone", using Mission Planner software.

### 2.2.1. Importing accurate elevation data

High quality elevation data at the correct spatial resolution is critical to determine the terrain-following flight path. An important feature for this purpose is to allow for the UAV (during autonomous operation) to climb or descend in a way that it maintains a specified distance above the terrain using external elevation data, which is provided by the ground control unit that is loaded to the autopilot prior to, or during flight.

#### Option1: Enhanced SRTM data for Scandinavia

The Shuttle Radar Topography Mission (SRTM) was flown aboard the space shuttle Endeavour in 2000. The U.S. agencies, National Aeronautics and Space Administration (NASA) and the National Geospatial-Intelligence Agency led the international effort to acquire radar data which were used to create the first near-global set of land elevations. SRTM successfully collected radar data over 80% of the Earth's land surface between 60° north and 56° south latitudes with data points every 1 arc-second (approximately 30 meters). Since northern parts of Scandinavia were not included, data compiled by *viewfinderpanoramas* was used. These data use Norwegian open survey data and are derived from 30-meter resolution datasets<sup>11</sup>. Using this data showed mixed results depending on where we tested flying, with non-acceptable results for Storlidalen, where the steep terrain requires more accurate altitude data.

#### Option 2: DEM data from the Norwegian mapping authority imported in Geotiff format

The Norwegian Mapping Authority (Kartverket) has an open and free web map service (Web Map Service, Figure 6) where DTM10 (Digital Terrain Model with 10 m resolution) data is available for the whole of Norway<sup>12</sup>. These terrain models can be downloaded in UTM33 projection (EUROEF89 UTM sone 33), with 10-meter resolution and can be exported as Geotiff format (see Figure 7). There is also a DTM1 terrain model, with 1-meter resolution which was acquired with airborne LiDAR<sup>13</sup>. A 0.25 m resolution DTM terrain model has also been tested on the Tiller test site. Each of the elevation models represents parts of Norway

<sup>11</sup> <http://viewfinderpanoramas.org/dem1.html>

<sup>12</sup> [http://sosi.geonorge.no/Produktspesifikasjoner/Produktspesifikasjon\\_Kartverket\\_DTM\\_20190815.pdf](http://sosi.geonorge.no/Produktspesifikasjoner/Produktspesifikasjon_Kartverket_DTM_20190815.pdf)

<sup>13</sup> <https://hoydedata.no/LaserInnsyn2/>

based on the WMS protocol, which is a standard protocol developed by the Open Geospatial Consortium in 1999 for serving georeferenced map images over the Internet<sup>14</sup>.

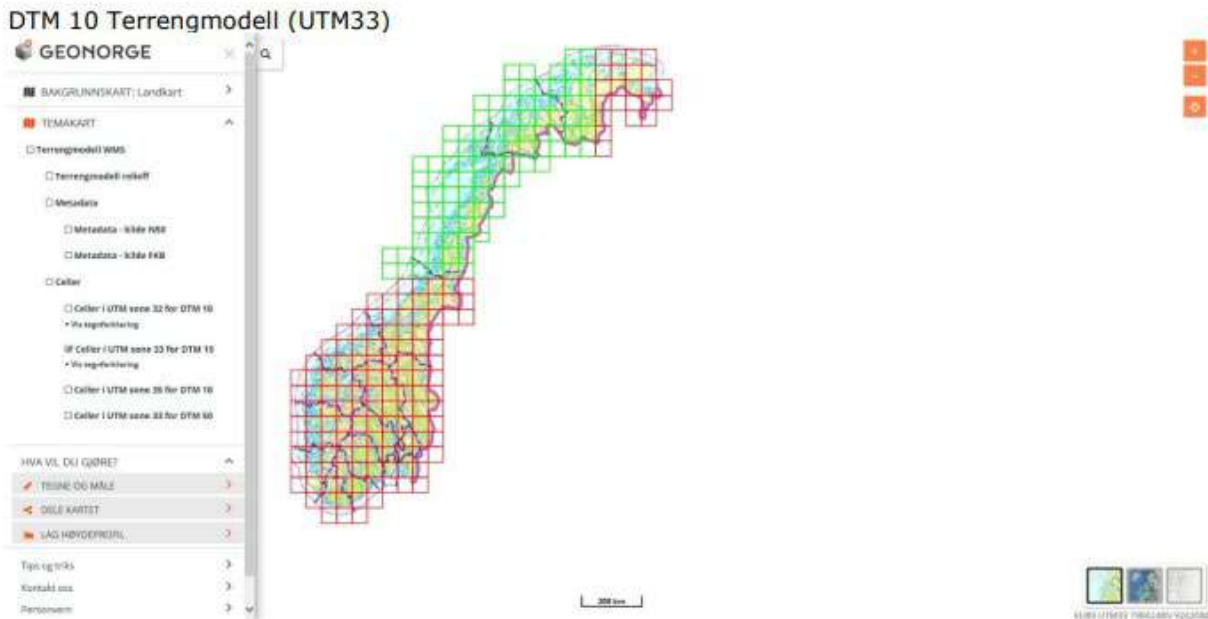


Figure 6. Web map service (WMS) from Kartverket<sup>15</sup>

Mission planner will automatically read the Geotiff files if it has the correct UTM (Universal Transverse Mercator) projection, which can be verified when planning a mission. The results will show rasterized elevation and terrain maps projected on top of the mission planning map (Figure 7).

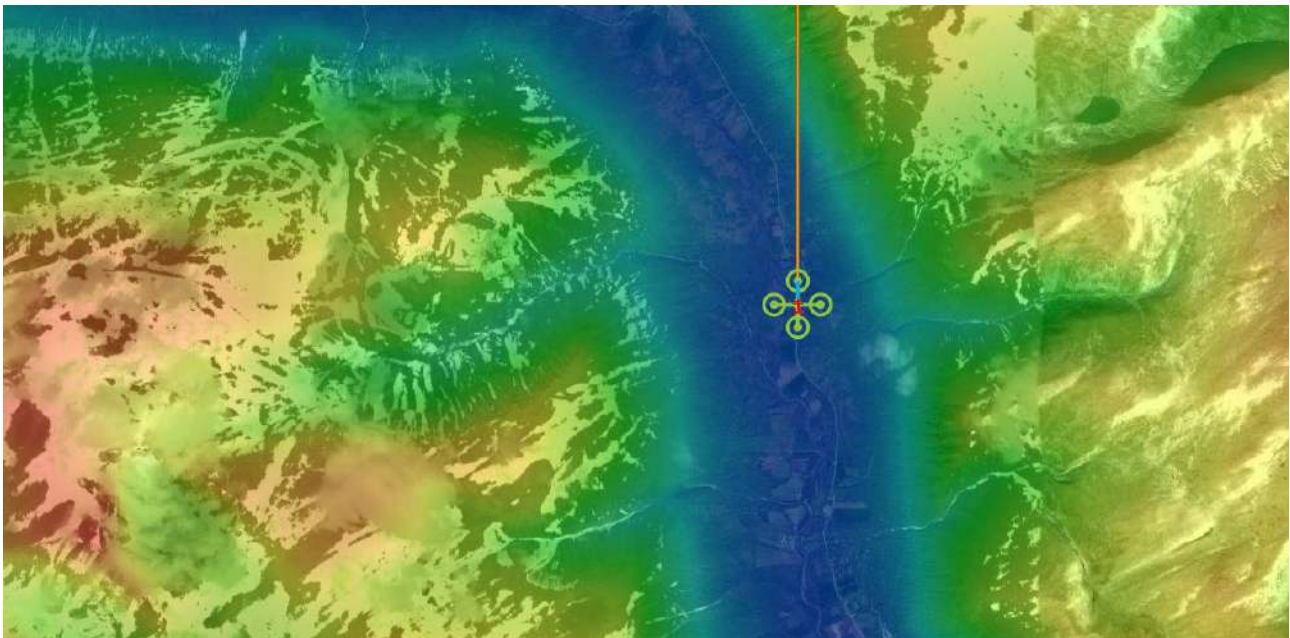


Figure 7. Satellite image with elevation overlay (blues = lows, reds = highs).

<sup>14</sup> Scharl, Arno; Klaus Tochtermann (2007). The Geospatial Web: How Geobrowsers, Social Software and the Web 2.0 are Shaping the Network Society. Springer. p. 225. ISBN 1-84628-826-6.

<sup>15</sup> <https://www.geonorge.no/>

Note that the actual terrain path is given by other specific parameters that need to be set in the autopilot, such as the distance between terrain grid points in meters. This controls the horizontal resolution of the terrain data that is stored on the flight controller and requested from the GCS. Note that in steep terrain, the interpolation needs to be sufficiently updated to provide adequate resolution. In this work, we have set the grid spacing to between 20 and 30 meters.

### 2.2.2. Dry run simulation of survey

When the survey is created, we implement a simulation feature in the workflow that can test that the flight is executed correctly according to the plan. An Ardupilot software-in-the-loop (SITL) simulator can accept the mission as if it was the actual UAV and be controlled externally from a GCS. This will reveal any possible problems with the actual flight path, which can be visualized in 3D (Figure 8).

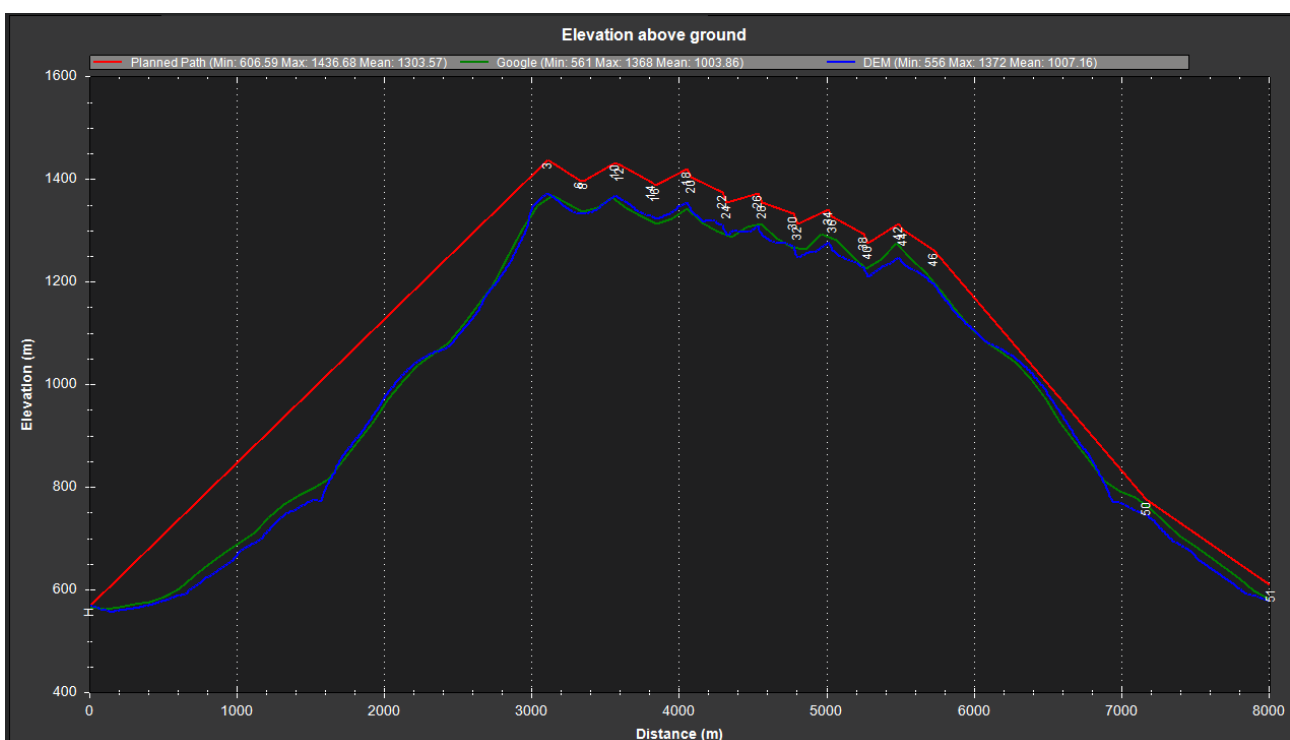


**Figure 8.** Elevation map of the generated survey, showing altitude above the terrain. Blue line represents elevation data from Google whereas the green shows imported data from Høydedata.no for Storlidalen. The red line displays the UAV planned flight altitude at a 100-meter surface altitude based on the imported DEM model from Høydedata.no.

The procedure is to load the survey into the virtual UAV over Mavlink, then start a mission, and review the log files. It is also possible to visualize the steps in real time. Additionally, if 3D maps are needed, the survey can be viewed over an API within a "Cesium Engine", where 3D maps are rendered live, which will not be explained in further detail here.



### 2.2.3. Terrain following optimization

A critical part of the flight planning and execution is to ensure that the elevation data accurately represents the terrain, and that the data is interpolated into the flight path correctly. To obtain an acceptable flight velocity vector, altitude points are used at a predetermined interval. The more often data is used for interpolating the flight path, the better the flight path will follow the actual terrain. On the other hand, if interpolation is coarser, the flight trajectory will be smoother, which may benefit the data capture processes, while conversely at the risk of not being able to correct sufficiently fast enough when there are significant changes in the terrain topography. A grid space compromise is necessary that is adequate and safe, while still ensuring that the UAV follows the terrain precisely. This is all automatically performed within the autopilot after parameter modifications in Ardupilot. In Figure 5, the planned path is shown for the Storlidalen survey, prior to flight. The final waypoint is at the end of the actual survey and does not include the complete return flight. Using a DEM10 accuracy terrain model, less than 100-meters terrain spacing should be used, especially if there are large elevation differences during the flight. It is shown that either 30- or 50-meters model will be adequate for this setup, but greater than the 100-meters model will cause a significantly lower flight path (see Appendix A for more details).

### 2.2.4. Run the survey in simulation

If the simulated run is successful and there are no issues with the survey plan, the survey is ready for execution on site. The pre-run shows that the survey follows the planned mission at the given elevation. Figure 9 shows a simulated survey over the Storhaugen avalanche starting zone. Flight durations are up to 35 minutes at a 10 m/s average speed over the survey site. Other examples of flight survey simulations are given in Appendix A, including tests with different terrain spacing (30, 50 and 100 m) for the background model used for the terrain following function.

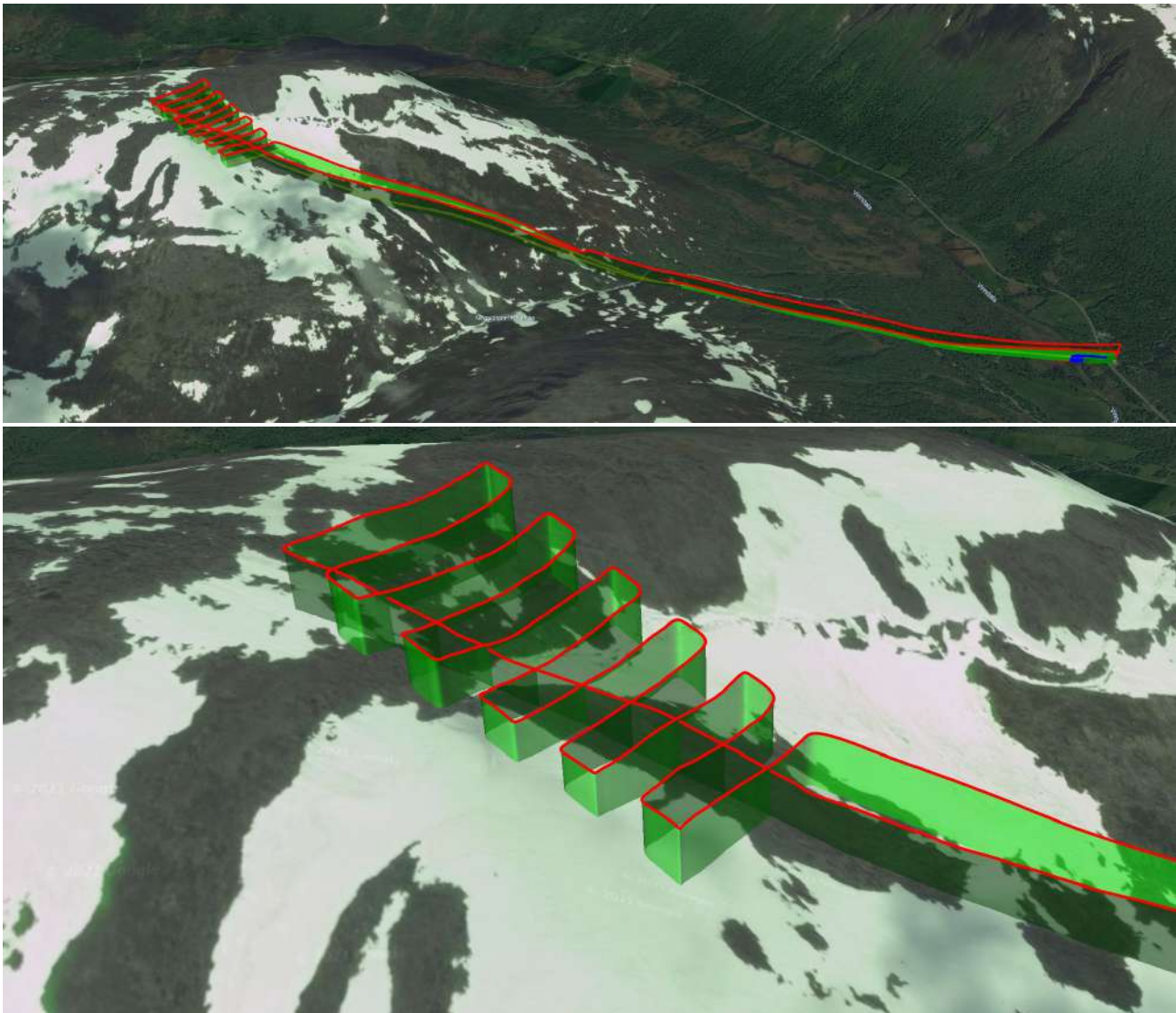


**Figure 9. Simulated flight where DEM (Digital Elevation Model) data corrects flight altitude (top). Zoom to the avalanche starting zone where the photogrammetry survey is performed (bottom). Target altitude is 100 meters above the terrain.**

### 2.2.5. Web application for flight execution

To simplify the procedures with executing a survey, and to create a starting point for automating and simplifying drone pilot workflow, a simple web application (app) has been developed with the sole purpose of starting a mission, as well as having the option to stop or abort the mission in case of an emergency. The idea is to keep the interface as simple as possible, intended for a hypothetical case of a user with minimal (or no) flight experience. One button starts the UAV and takes it to an altitude of 5 meters. The second button commands the flight plan to start the mission (Figure 10). The UAV can be controlled with this app. Additionally, if necessary, current flight paths, progress, and other data can be monitored in an additional GCS, such as Mission Planner software. For redundancy in this setup, a radio-controller is connected through an independent radio link, which enables secondary control of the UAV by direct RC-control.



**Figure 10. Preliminary ground command application to simplify mission control and for scheduling flights.**

### 2.2.6. Degree of autonomy

The UAV autonomy is primarily focused on drone safety and not on real-time intelligent flight systems. This setup ensures flight autonomy based on a pre-defined flight path. As the Ardupilot autopilot has multiple layers of fail-safe routines configured, the UAV will be able to safely abort mission if needed, based on several sensors and system monitors. The system with the web app can be set up to run at given time schedules, for example execution of a flight at a time when blue skies are forecasted (Figure 11). This has been tested with some of our UAVs "remotely", i.e., the user is running the app online, while a second pilot is performing flight supervision on site. This conceptually opens for remotely supervised or repeatable scheduled flights based on time intervals, or other events. This has been tested for flights where the UAV is set up to run photogrammetry flights starting every hour. A survey is then performed once the clock reaches the given start time (at the stroke of a new hour). The application "listens" to the flight, to ensure that only one flight order can be given at a time. This opens also for repeatable flights so that a timer can be set to run the UAV a given time interval after it lands from its previous flight. Additionally, a new survey is only allowed at a set battery voltage, ensuring that missions have minimum adequate battery power. The app was programmed in python using the pymavlink<sup>16</sup> library to communicate with Ardupilot.

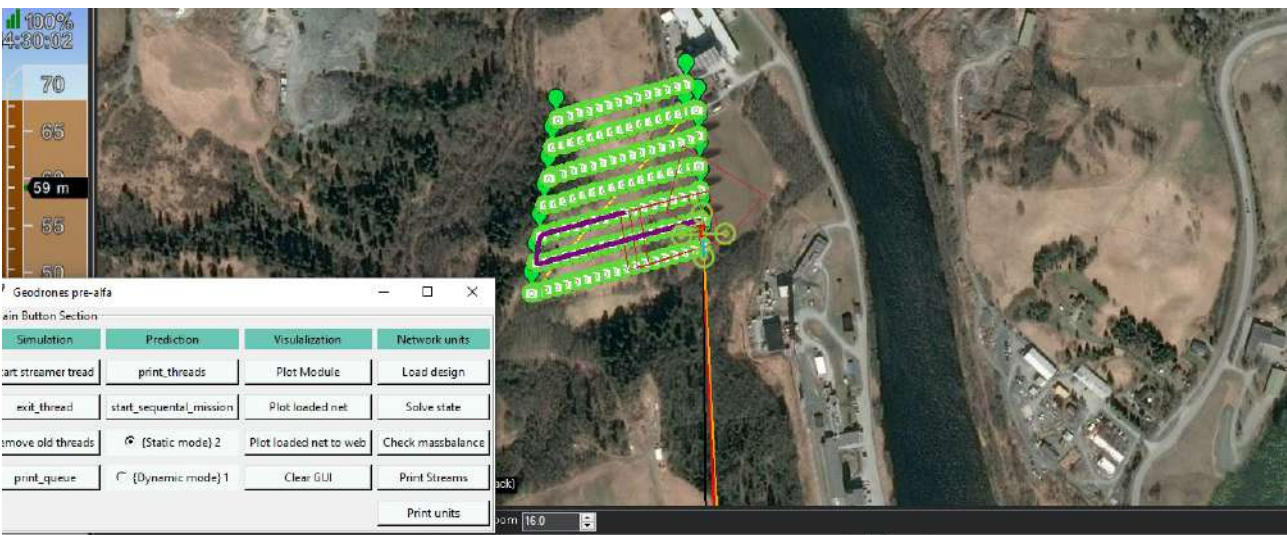


**Figure 11. Flight that is executed at pre-set time schedules (Mission Planner software shown in the background).**

<sup>16</sup> <https://github.com/ArduPilot/pymavlink>

## 2.3. Data/images recording

The UAV collects a set of optical images at intervals determined by the flight plan such as survey pattern, altitude, speed and camera type. When the flight controller requests an image, the camera shutter is triggered and a hot shoe sensor on the UAV registers the corresponding time stamp and the current GPS position. In this case, the optical sensor is mounted nadir, so it does not require any extra angle correction. In the case of off-nadir mounting or gimbal mounting, extra corrections need to be applied to georeferenced images. At the end of the survey, a set of images (often several hundred) are stored on the camera's SD-card. The first post-process is to geotag the images according to the time stamp events, followed by running the image set through photogrammetry software to create a 3D model of the survey area.

### 2.3.1. Georeferencing UAV images

The UAV uses a dual GPS-system, where the master GPS is a multi-band RTK-GNSS receiver that allows for centimeter precision. The second GPS allows for redundancy. The setup consists also of a base station that is used for RTK corrections, which ensures real time updating of position, or a post processing kinematic (PPK) correction workflow. The PPK solution is efficient and fast and does not require an RTK correction feed during mission. Alternatively, PPP (precise point positioning) can be used.

### 2.3.2. PPK workflow for georeferencing

When the mission has been completed, there will be log files available in both the Rover (UAV) as well as the base station. The workflow for georeferencing consists of the following:

1. Downloading both logs by logging on to the Wi-Fi network of the respective units. Prototype One uses the Emlid Reach RS2 as Base, with the Reach M2 multiband on the Rover.
2. The most convenient way is to log the .UBX files, which contain raw files and trigger points during flight giving exact location during image acquisition through the hot shoe sensor.

### 2.3.3. Creating batch data workflows

Typically, the images are loaded onto an SD card on the UAV, which must be transferred, preferably by Wi-Fi, to a data uploader unit for further processing or directly through 4G/5G network. Experimental testing has been performed with a single board Linux computer that is connected to the server via 4G mobile connection (Figure 12). The concept is based on the need for an operator to load up data to a processing server while being in the field, and after the images have been loaded from the UAV (to the uploader).

# Field data uploader prototype

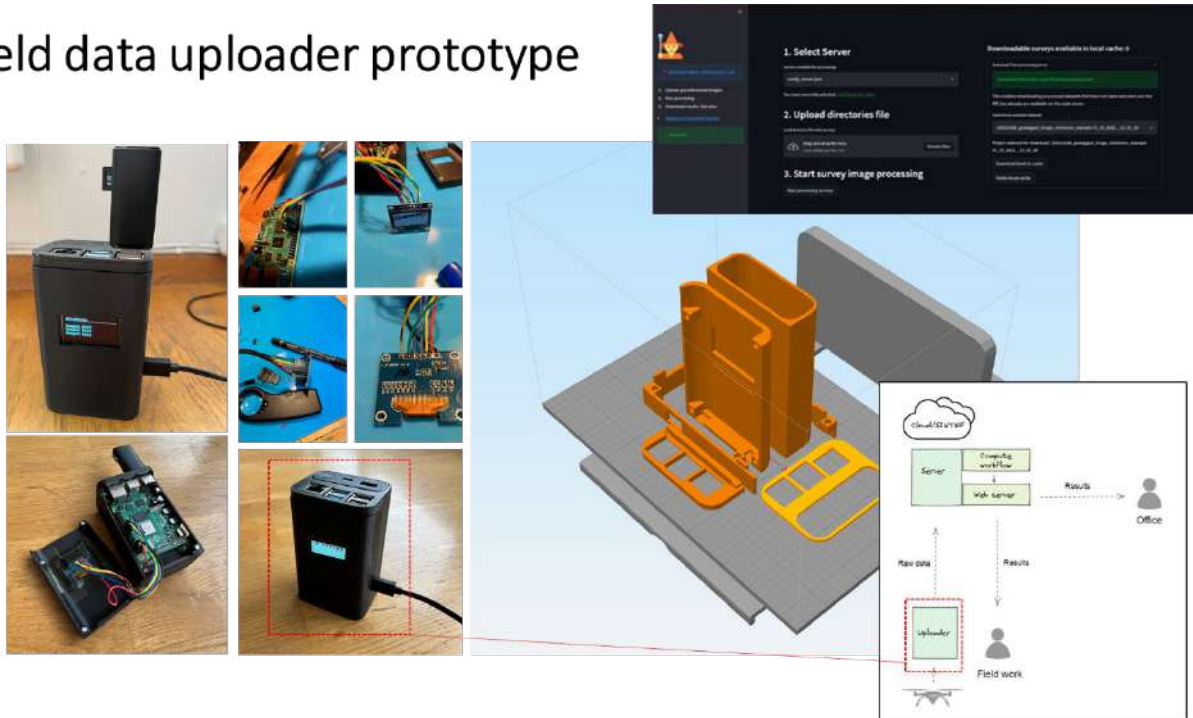


**Figure 12. Prototype of the data uploader unit. The client runs on the unit, which uploads all files in a directory and can be subsequently handled in a cloud computing environment.**

## 2.4. Data processing with open-source software

### 2.4.1. Photogrammetry workflow

Photogrammetry relies on the principles of optics and knowledge of the interior geometry of the camera and its relative orientation, to reconstruct dimensions and position of objects represented within the images taken. The most frequent application of photogrammetry is the analysis of stereo aerial photography to derive estimates of the topographic elevation. With the aid of accurate real time positioning GPS systems and/or local information such as ground control points (GCPs), highly accurate topographic models can be created. Using specific software running on high performance workstations, accurate digital elevation models (DEMs) and point clouds can be created. We describe here an automated workflow over a web-enabled API so that surveys comprising hundreds of images can be processed automatically.

While commercial software packages offer user-friendly image processing approaches, the flexibility, availability, and maturity of open-source software could be a key to developing useful solutions that require access to the details of the code. It also allows to optimize the combination of different packages in an integrated workflow to tailor for a particular application. Some examples of open-source software and libraries include MicMac<sup>17</sup>, VisualSfM<sup>18</sup>, Bundler<sup>19</sup>, Python Photogrammetry Toolbox<sup>20</sup>, OpenSfM<sup>21</sup>, OpenMVS<sup>22</sup>, PDAL<sup>23</sup> and Entwine<sup>24</sup> and Open Drone Map<sup>25</sup>, which are all based on Structure-from-Motion algorithms. Among the different photogrammetry packages freely available, Open Drone Map is the processing software that is used in the most recent work. This package utilizes several other active open source projects, such as the mentioned OpenSfM, OpenMVS, PDAL, Entwine and MicMac. We created an independent server application to communicate with the NodeODM API.

When georeferenced images are ready for further processing, the survey image set can be uploaded to the SfM-server from a field client. The purpose of this task is to generate georeferenced maps of the surveyed area, DEMs and textured 3D models and point clouds. To enable use of this workflow, we developed an external client that can communicate with the server through a RestAPI-interface, for automatic uploading of data to server and image processing. The client is set up containing two configuration files.

1. The configuration and credentials to the server.
2. List of paths to directories where images from surveys are located, for example for the batch list of 13 surveys in Figure 13.

The client will upload the images to the server and run the processing according to a configuration file, specifying the parameters for the photogrammetry. The workflow is summarized in Figure 14.

---

<sup>17</sup> MicMac (<https://micmac.ensg.eu/>)

<sup>18</sup> VisualSfM (<http://ccwu.me/vsfm>)

<sup>19</sup> Bundler (<https://www.cs.cornell.edu/~snaveily/bundler>)

<sup>20</sup> Python photogrammetry toolbox (<https://github.com/decentropy/photogrammetry>)

<sup>21</sup> OpenSfM (<https://opensfm.org/>)

<sup>22</sup> Open Multi-View Stereo reconstruction (<https://github.com/cdcseacave/openMVS>)

<sup>23</sup> Point data abstraction library (<https://pdal.io/>)

<sup>24</sup> Entwine (<https://entwine.io/>)

<sup>25</sup> Open drone map (<https://www.opendronemap.org>)

```

1  D:\statens_vegvesen\Bispefonna\2021\20042021
2  D:\statens_vegvesen\Bispefonna\2021\27052021
3  D:\statens_vegvesen\Bispefonna\2021\30042021\Bilder
4  D:\statens_vegvesen\Bispefonna\2021\27052021
5  D:\statens_vegvesen\Fv63Stavbrekkfonna\100_0348
6  D:\statens_vegvesen\Fv63Stavbrekkfonna\100_0349
7  D:\statens_vegvesen\Fv63Stavbrekkfonna\100_0351
8  D:\statens_vegvesen\Fv63Stavbrekkfonna\100_0352
9  D:\statens_vegvesen\Fv63Stavbrekkfonna\100_0353
10 D:\statens_vegvesen\Fv63Stavbrekkfonna\100_0355
11 D:\statens_vegvesen\M300_Breiddalen1_gsd2_o80_s70
12 D:\statens_vegvesen\P4_Grasdalen1_gsd2_o80_s70
13 D:\statens_vegvesen\Trollstigen\02_Bilder_2015
  
```

Figure 13. Example of input text file with the list of surveys to complete as one processing job

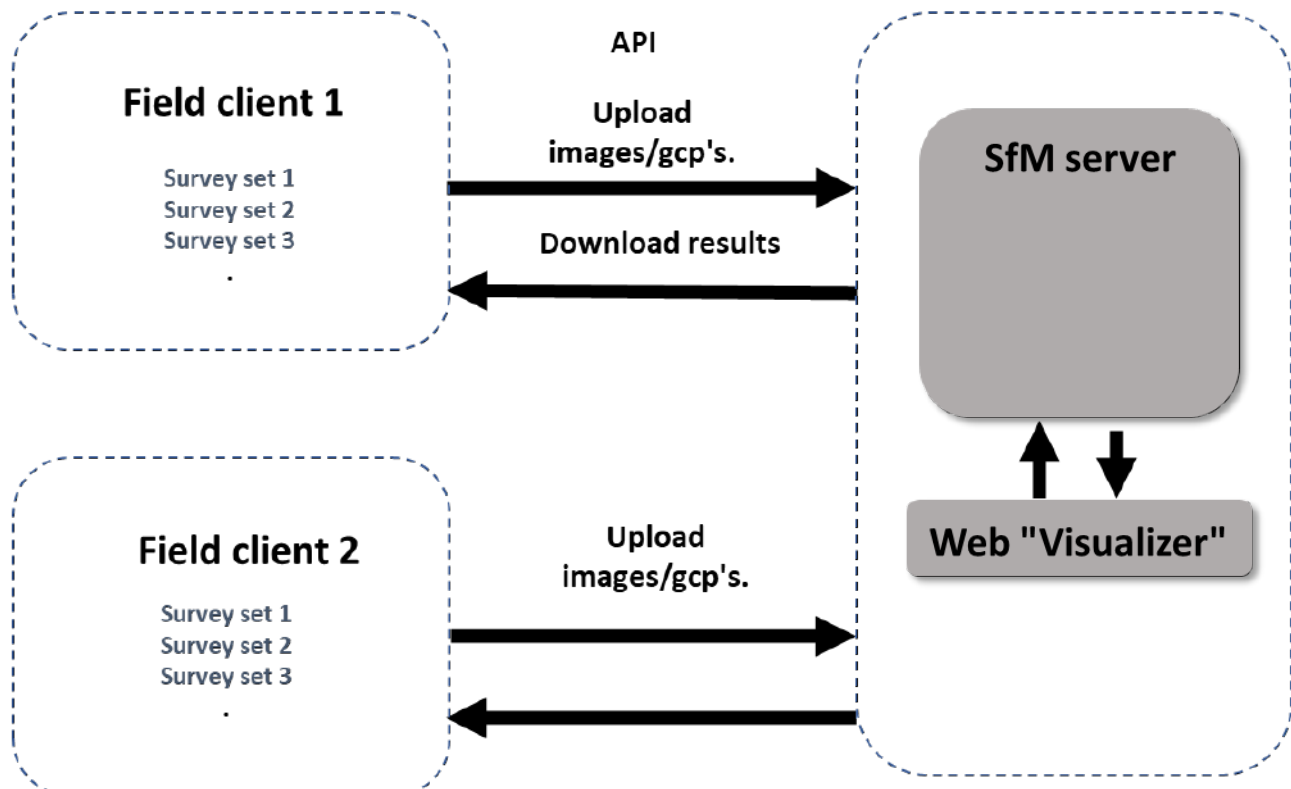


Figure 14. Schematic of the client server communication

When the processing is finished, the client can alternatively download results from the selected surveys. The uploader API can also function as a standalone webpage, that can run on a client computer or a server. All image sets can thus be uploaded directly from the webpage or from the field data uploader unit (based on a Raspberry pi computer). When the processing is finished, the results are downloadable as a "one-click" operation. Alternatively, an auto forward function can send the results over a request API once processing is completed (the last feature is currently not tested in this test workflow).

## 2.4.2. Georeferencing, change detection and data interpretation

Change detection and estimation of snow height above terrain are important pieces of information to gather with other data, to help in estimating the avalanche hazard for a given area. We have used the following procedures to create the canopy model which gives the difference between two raster layers, i.e., snow height changes. To produce the point clouds, the 16-bit Tiff orthophotos and the elevation models, the stages need to be carried out in a streamlined, preferably automated, fashion to ensure dataset repeatability. This reduces workloads as well as manual steps that may be prone to error. We have used QGIS software<sup>26</sup> with its API allowing for automated scripting.

High-resolution (primarily snow-free) elevation maps are available for all of Norway<sup>27</sup>. For the explanatory test case described here, the Tiller area was used for survey testing and testing georeferencing accuracy. For the test site, DEM10 model with 25 cm resolution is available. This level of detail is not always available, especially in remote areas. The maps in Figures 15 and 16 show hillshades (shaded relief maps) of surface and terrain models, respectively.

Prosjekt/datasett: Trondheim 5pkt 2017, Oppløsning: Som kildedata, Format: GeoTIFF, Kompresjonsmetode: LZ77, Produkt: DTM



**Figure 15. Surface elevation map from airborne LiDAR**

<sup>26</sup> <https://qgis.org/en/site/>

<sup>27</sup> [www.hoydedata.no](http://www.hoydedata.no)



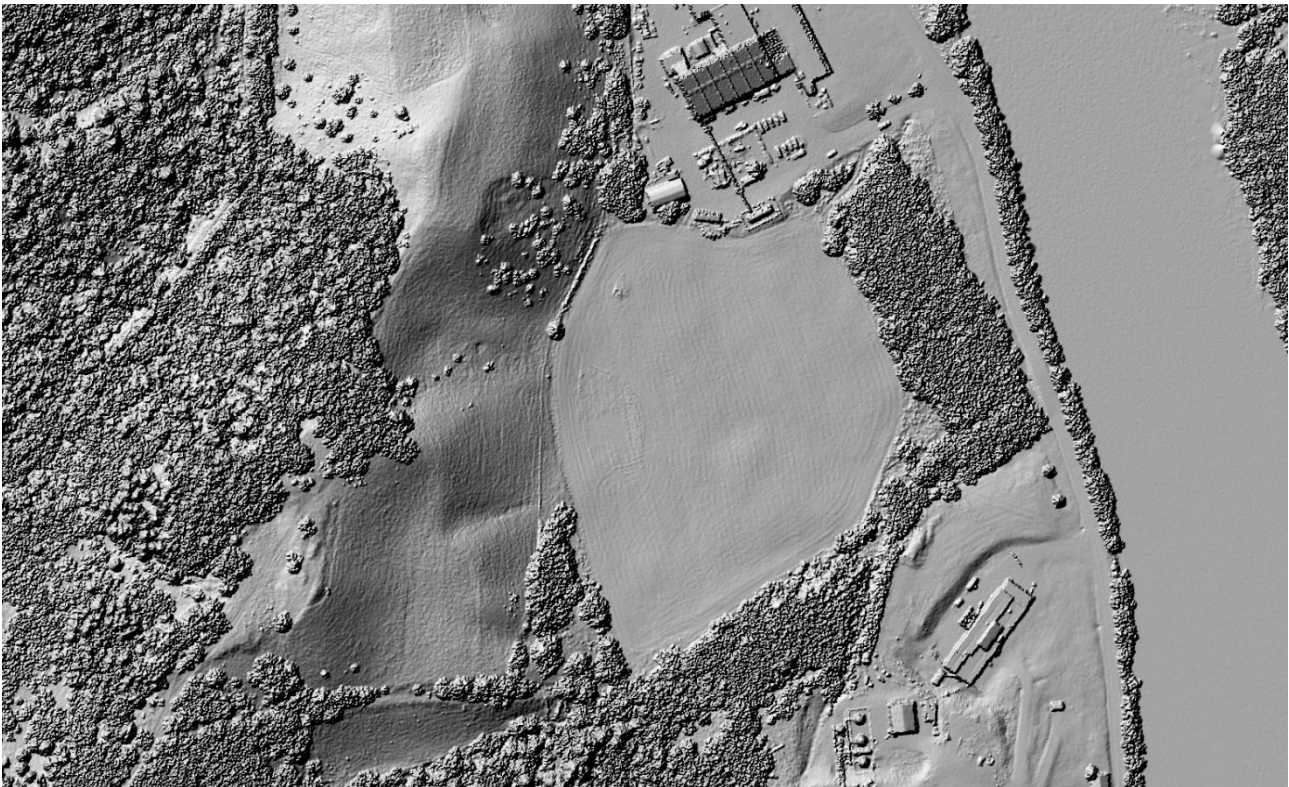


**Figure 16. Terrain elevation map from airborne LiDAR**

The coordinate reference system used for the test case was EPSG 25832-ETRS89 32N or EUREF89, which is also what is used for all layers, which has a limited accuracy of at best 0.1 meters. The vertical reference uses Normal Null 2000 (NN2000). All models created from the UAV data consequently need to be converted to the same coordinate reference system both horizontally and vertically.

The UAV photogrammetry models are already georeferenced, with a different projection. This needs to be converted to the given standards. For all UAV-created models, we follow this procedure:

1. Convert to NN2000, a free reference model can be found online<sup>28</sup>
  - a. In QGIS, the raster calculator is used to reproject the elevation according to the NN2000 reference height.
  - b. Subtract the DSM (Digital Surface Model) from the NN2000 model.
  - c. Create a vector shape from the raster image which is then reprojected.
2. The processed geotagged images are in standard ellipsoidal projection (WGS), which needs to be reprojected to ETRS89 32N.
  - a. Reproject raster using the QGIS reprojection GDAL function.

<sup>28</sup> <https://www.agisoft.com/downloads/geoids/>

### 2.4.3. Validations at Tiller test site

#### **Camera specification and image overlap**

Tests were conducted with different camera settings on the Sony  $\alpha$ 6000. Optimum image quality was found at Aperture Priority mode [A] at ISO 100, with a set aperture of about f/2.8-f/2.1. The testing was performed in overcast weather, and the setting aperture was set manually. GCPs (Ground Control Points) were used for georeferencing validation, and the spatial error was reasonably low and limited by the accuracy of the current GPS-setup and UAV speed (5 m/s).

Ideally, GCPs should be measured to calibrate the camera and UAV setup, but this is not always available, and is unpractical and unsafe in steep terrain. It is therefore important to assess what the estimated accuracy was for the RTK setup. In general, the average errors were in the range of 20-30 cm. The flights were approximately 5 minutes in duration. The UAV has the capacity to fly up to 50 minutes, which means that quite large areas can be covered, or alternatively longer transport flights before the survey can be taken (see e.g., Figure 9).

#### **Processing and post-processing workflow**

Below are presented logs from two missions as examples without detailed analysis given. The largest survey, Mission 5, captured 280 images, and is further discussed. The reference comparison was based on a UAV flight performed at 60-meter altitude above ground surface, and the intention was to run a fast flight for quick rendering of images on the cloud server. Some summary data from the processing are as follows:

- Final GSD: 1.44 cm, RTK-FIX 100%, NTRIP corrections from Saupstad base (Trondheim).
- Camera options: set aperture.
- Flight time: 4 minutes 55 seconds.
- Area: 1.18 km<sup>2</sup>.
- Terrain following altitude: 60 m.
- Vehicle: Geodrones Prototype One.
- Payload: RGB camera Sony RX120.

Figures 17 to 20 show examples of results at Tiller test site including change detection maps showing snow melting.

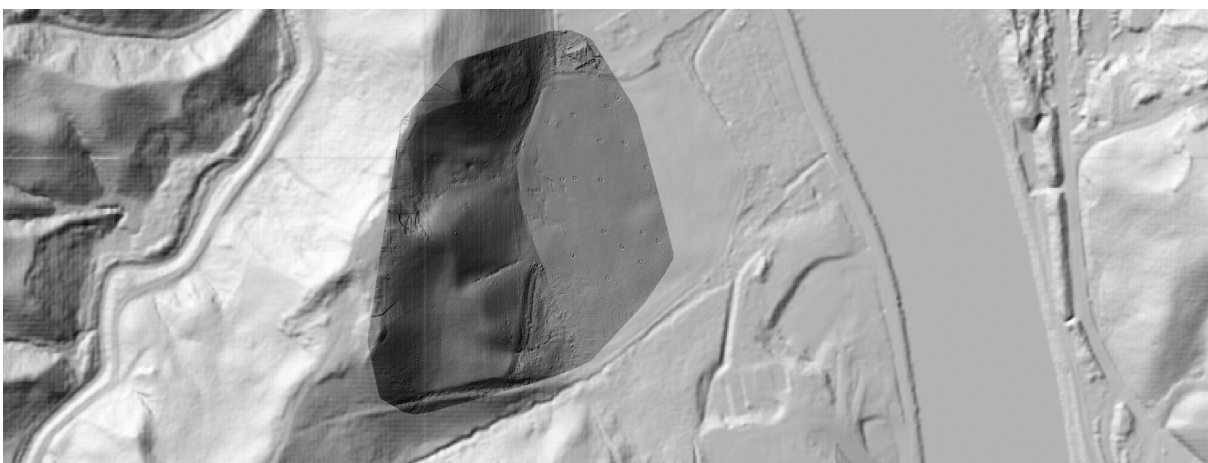


**Figure 17. Projection to Euref89, 25 cm increment resolution DEM, with drone layer on top of raster. The darker zone highlight the change detection zone used in Figures 19 and 20.**



**Figure 18. Rendered point cloud model.**

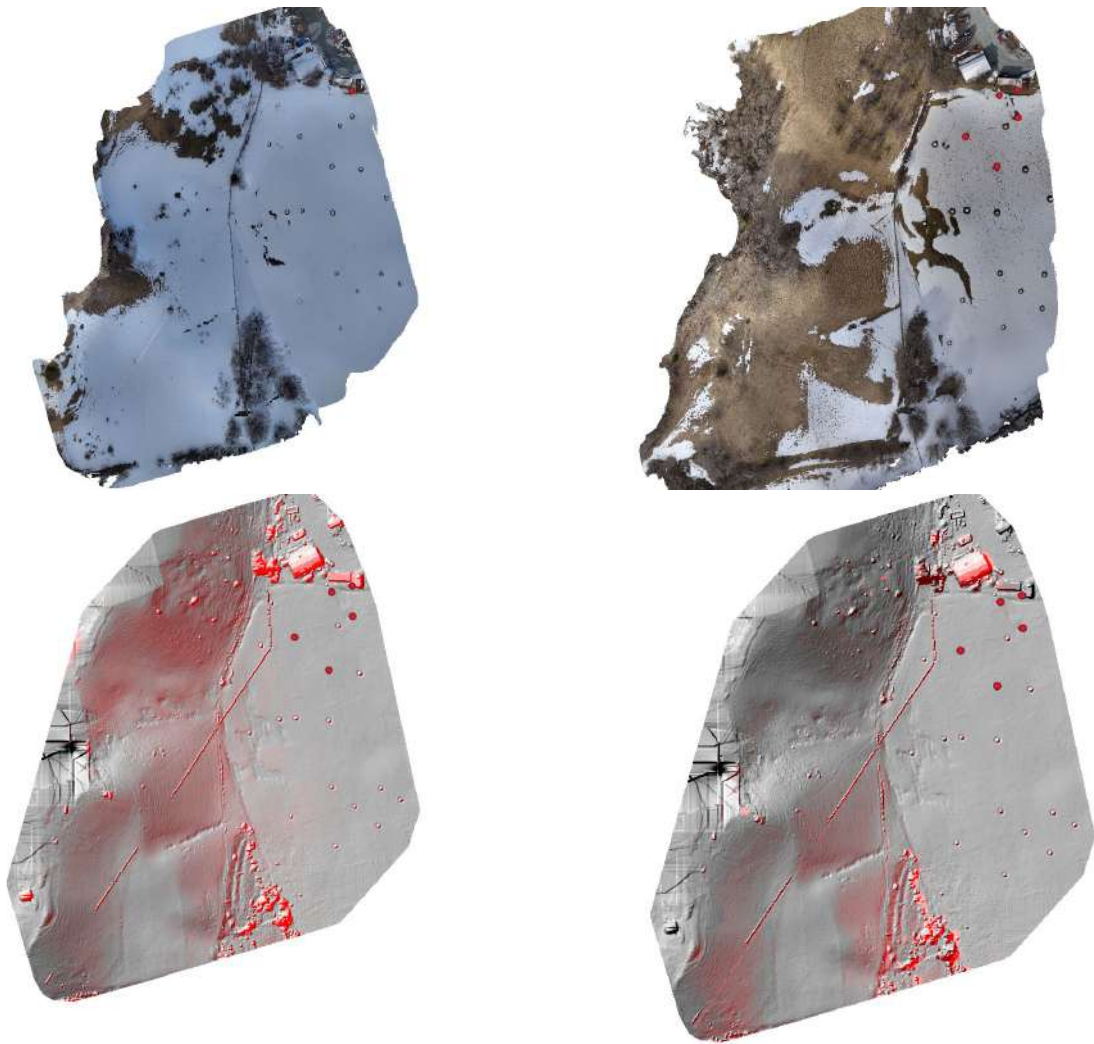


**Figure 19. (Top) rendered orthophotos and (Bottom) hillshades with qualitative change detection relative to the reference layer (airborne LiDAR), Surveys performed 7 days apart, showing snow melting (first survey on the left, second survey on the right).**

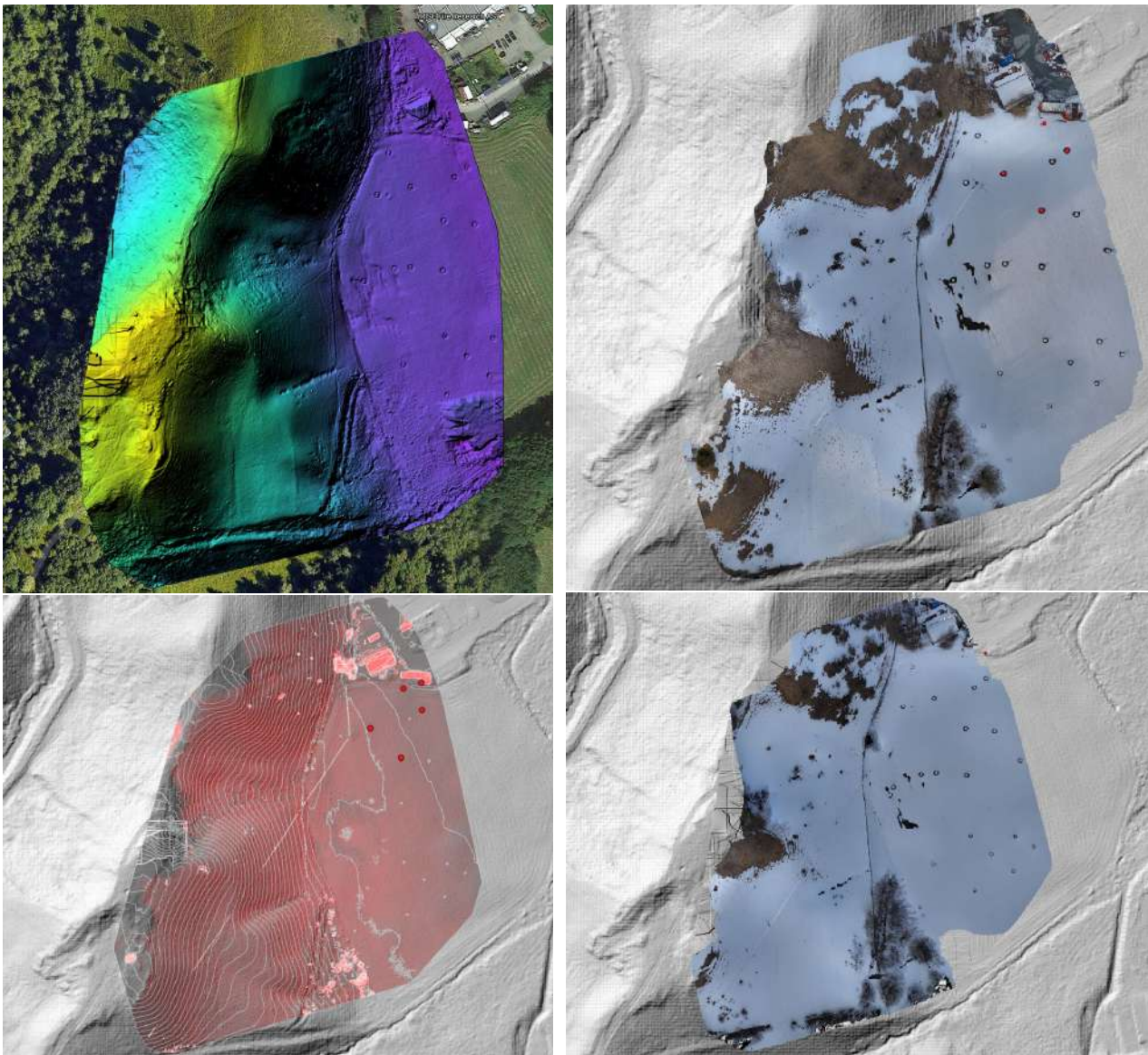


**Figure 20. Additional visualization of the rendered orthophotos and hillshades background and with change detection relative to the reference layer (from airborne LiDAR). From two different "quick surveys" one week in between.**

#### ***Ground control points (GCPs)***

GCPs were set up for comparison with the multiband RTK-GPS system in a PPK procedure. Corrections were taken from a local NTRIP-provider. The base station reference point was therefore set up with potential centimeter absolute horizontal positional accuracy.

#### ***Survey errors***

Calculated accuracies are provided for photogrammetry results for GPS and GCPs if used. The absolute errors were in the range of 25 cm for the vertical accuracy.

Additional examples of processing of photogrammetry datasets with this open-source implementation are given in Appendix B whereas full scale surveys above avalanche starting zones are processed automatically to derive orthophotos, point clouds and DEM.

## 2.5. Data processing with commercial software

### 2.5.1. Photogrammetry workflow

Several commercial photogrammetry software packages are available, some of which use local processing resources and a one-time purchase price, while others use cloud-based processing resources and require subscription-based or per-use fees. Among the most widely used commercial software packages are Pix4Dmapper (Pix4D SA, Lausanne, Switzerland)<sup>29</sup>, Agisoft Metashape (Agisoft LLC, St. Petersburg, Russia)<sup>30</sup>, DJI Terra (SZ DJI Technology Co., Ltd., Shenzhen, China)<sup>31</sup> and DroneDeploy (DroneDeploy, Inc., San Francisco, CA, USA)<sup>32</sup>.

Generally, all software packages use a Structure-from-Motion Multi-View Stereo photogrammetry workflow, for which the general steps are:

1. Bundle adjustment (image alignment, estimation of camera parameters)
2. Depth mapping
3. Dense point cloud generation
4. Surface meshing
5. Textured model generation

Each software package offers a user manual that describes a step-by-step approach for the processing workflow. Many of the processing steps are possible to automate, however, manual intervention may be necessary to e.g., trim point clouds before generating mesh surfaces, or to verify ground control points (if used). Dense point clouds are usually filtered, based on statistical confidence, and resampled, based on desired point spacing. Georeferenced dense point clouds and tiled models are typically exported for further interpretation in other software.

---

<sup>29</sup> <https://www.pix4d.com/product/pix4dmapper-photogrammetry-software/>

<sup>30</sup> <https://www.agisoft.com/>

<sup>31</sup> <https://enterprise.dji.com/dji-terra>

<sup>32</sup> <https://www.dronedeploy.com/>

### 3. Recommendations for flight planning and autonomous data collection – LiDAR

#### 3.1. General workflow and hardware

This section describes the main steps in performing UAV LiDAR scans of snow surface terrain. The aim of the workflow presented herein is to generate digital terrain models with sufficient quality for supporting daily, local avalanche hazard forecasts. To achieve useable data products for the avalanche forecasting use case, several computing steps are required, including some manual intervention. For example, manual quality control is needed if the terrain includes different surface types. Flight mission planning, data pre-processing, filtering and classification of the resulting point clouds are described. In the GEOSFAIR project, commercial-off-the-shelf UAV are used to collect data. The DJI Matrice 300 RTK aircraft, equipped with the Zenmuse L1 LiDAR scanner is the main system used to collect LiDAR data. The technical specifications for the UAV and the LiDAR sensor are listed in Table 1 and Table 2, respectively.

**Table 1. Technical specifications for the UAV DJI M300**

<b>Weight (with single downward gimbal)</b>	Approx. 3.6 kg (without batteries) Approx. 6.3 kg (with two TB60 batteries)
<b>Max Payload</b>	2.7 kg
<b>Max Takeoff Weight</b>	9 kg
<b>RTK Positioning Accuracy</b>	When RTK enabled and fixed: 1 cm+1 ppm (Horizontal) 1.5 cm + 1 ppm (Vertical)
<b>Max Wind Resistance</b>	15 m/s
<b>Max Flight Time</b>	55 min
<b>Ingress Protection Rating</b>	IP45
<b>Operating Temperature</b>	-20°C to 50°C (-4°F to 122° F)

**Table 2. Technical specifications for the DJI Zenmuse L1 LiDAR scanner**

<b>Name</b>	Zenmuse L1
<b>Weight</b>	Approx. 900 g
<b>Power</b>	30 W
<b>IP Rating</b>	IP44
<b>Operating Temperature Range</b>	-20° to 50° C (-4° to 122° F)
<b>Detection Range</b>	450 m @ 80% reflectivity, 0 klx; 190 m @ 10% reflectivity, 100 klx
<b>Point Rate</b>	Single return: 240,000 pts/s; Multiple return: 480,000 pts/s
<b>System Accuracy</b>	Horizontal: 10 cm @ 50 m; Vertical: 5 cm @ 50 m
<b>Ranging Accuracy</b>	3 cm @ 100 m
<b>Maximum Returns Supported</b>	3
<b>Scan Modes</b>	Repetitive line scan mode, non-repetitive petal scan mode
<b>FOV</b>	Repetitive line scan: 70.4°×4.5° ; Non-repetitive scan: 70.4°×77.2°
<b>Laser Safety</b>	Class 1
<b>IMU Update Frequency</b>	200 Hz
<b>Accelerometer Range</b>	±8 g

Angular Velocity Meter Range	±2000 dps
Yaw Accuracy	Real-time: 0.18°, Post-processing: 0.08°
Pitch / Roll Accuracy	Real-time: 0.03°, Post-processing: 0.025°

### 3.2. Flight planning

Flight planning in UAV operations typically begins with designing flight lines within an area of interest, but requires additional considerations which add to the complexity of flight planning. Flights need to be in accordance with the national rules and regulations for operating UAVs. In addition, the UAV operating organization may have an additional set of requirements to be followed. This section describes the major steps that are needed to fulfill the UAV flight requirements. The list has a numbered order, which is practical for most use cases:

1. Apply for specific category operation in [airdata.com](https://airdata.com) (NPRAs flight log system), if needed (e.g., in case of BVLOS flights).
2. Draw/import polygons of interest in Google Earth and export as keyhole markup language (KML) file.
3. Import polygons of interest into DJI FlightHub 2 (Figure 21). This step is not mandatory but provides the operator with a good overview of the flights, while also enabling the flights to be live monitored from the office. Flight polygons can also be imported to the remote controller from DJI FlightHub 2, or directly drawn in the remote controller interface.



Figure 21. Three flight polygons in Grasdalen, along highway Rv15. Screenshot from DJI FlightHub 2.



4. Upload terrain model to the remote controller. In Norway we use the national map services providing data derived from airborne LiDAR<sup>33</sup>. Convert the terrain model to datum: WGS84/ellipsoidal height. Alternatively, download terrain model in DJI Pilot 2 app on the remote controller (ASTER data). This latter option is a less accurate terrain model, but often good enough.
5. Apply desired mission settings in the Pilot app on remote control. For measurements in steep snow-covered terrain, the typical mission settings are listed in Table 3. The flight lines are illustrated by an example in Figure 22.

**Table 3. Desired flight settings applied in the DJI Pilot 2 application.**

<b>Settings in the DJI Pilot 2 app on remote controller</b>	
IMU Calibration	ON
Terrain follow	ON
Terrain following height	40-100 m
Flight speed	7-10 m/s
Elevation optimization	OFF (only needed for photogrammetry)
Upon Completion	Exit task
<b>Advanced settings</b>	
Side Overlap	30-50 %
Forward overlap	50 % (only needed for colorizing of point cloud)
Course angle	Depends on the terrain. Avoid flying up and down the slope.
Margin	0 m
Photo mode	Timed Interval Shot
<b>Payload settings</b>	
Return mode	Dual
Sampling rate	240 kHz
RBG Coloring	ON

<sup>33</sup> <https://hoydedata.no/LaserInnsyn2/>



**Figure 22. Flight route while LiDAR scanning desired polygon (blue). Flight lines are colored according to colorbar illustrating altitude above sea level (meters).**

6. Fill out preflight checklist.
7. Fly up to start point for the mission, not exceeding 120 m altitude above ground surface. This fly-to-start step can be performed either manually, or by adding a flight mission from home point to mission start point.
8. Perform mission flight, while monitoring UAV safety parameters. Control the point cloud acquisition during flight on the live point cloud display.
9. Return to home point either by flying manually or by adding a return flight mission. Do not exceed 120 m altitude from nearest ground surface.
10. Perform post flight check list.

### 3.3. Data processing

Recorded LiDAR data with DJI Zenmuse L1 sensor needs to be processed in proprietary software, DJI Terra. The typical output format from DJI Terra is LAS files. Every point cloud viewer/editor software can open these LAS files for post processing, classification, and filtering. Recommended settings for generating point clouds in DJI Terra are listed in Table 4.

**Table 4: Point cloud processing settings in DJI Terra.**

<b>DJI Terra settings</b>	
Point cloud density	By Percentage (100 %)
Point cloud processing	Optimize Point Cloud Accuracy (the other checkboxes are unchecked. Smoothing and cloud classification are taken care of in post processing.)
Output coordinate system	Horizontal: ETRS89 / UTM zone 33 (central Norway) Vertical: NN2000 (Norway)

The resulting LAS files can be used directly in calculations or for visualization, but further processing is usually needed. Depending on the desired output, further processing can include different types of point filtering and noise removal, point classification and strip adjustment to improve the consistency between adjacent flight lines. Examples of software commonly used for point cloud processing are CloudCompare (free, open source)<sup>34</sup> and Terrasolid (Terrasolid Ltd., Espoo, Finland)<sup>35</sup>.

In this project, the final processing was automated using a scripted tool in ArcGIS Pro<sup>36</sup> (Table 5). To minimize the processing time, only ground classification was performed before DSM was produced. The DSM was then compared to DSMs from previous scans to calculate changes. This simplified procedure was found to work well, even for snow-covered terrain, but could lead to noise and errors in cases with more vegetation or steeper terrain.

**Table 5: Automated processing steps in ArcGIS Pro.**

Step	Tool	Description
Point cloud classification	Classify LAS Ground	Method: Aggressive DEM resolution: Undefined (no subset used)
Filter point cloud	Create LAS Dataset Make LAS Dataset Layer	Create layer from ground points only (class code=2).
Calculate cell size		Minimum cell size = 4 * average point spacing
Create DSM	LAS Dataset to Raster	Value: Elevation Interpolation type: Binning, average, simple Sampling type: Cell size Sampling value: Calculated cell size
Add DSM to source mosaic dataset	Add Rasters to Mosaic Dataset	DSM saved as .tif to network drive and added to the source mosaic dataset.
Resample DSM	Resample	Resample DSM to cell size = 0.5 m. Resampling type: Bilinear.
Create snow height map	Raster calculator	Snow DSM minus snow free DTM at 0.5 m resolution.
Create snow height change maps	Raster calculator	Snow DSM minus previous snow DSMs (last, 1 day and 3 days).
Add results to source mosaic	Add Rasters to Mosaic Dataset	Snow height and snow height change maps saved as .tif to network drive and added to the source mosaic dataset.

### 3.3. Publishing of results

The final products presented to forecasters should include a shaded relief map showing snow surface structures, as well as snow height above terrain and snow height change maps. Additional products that can be useful are snow surface slope maps and, potentially, highlighting of important features in the map products. If the results will only be published online, it is recommended to use raster functions to derive raster products on-the-fly to limit the amount of stored data.

In this project, results were made available through a set of derived mosaic datasets published to an ArcGIS image server. Raster functions were used to generate shaded reliefs, while the other products were published as individual TIF files. The published map services were presented to forecasters in a simple web application based on the imagery viewer available from ArcGIS Instant Apps.

<sup>34</sup> <https://www.danielgm.net/cc/>

<sup>35</sup> <https://terrasolid.com/>

<sup>36</sup> <https://www.esri.com/en-us/arcgis/products/arcgis-pro/overview>

### 3.4. Data validation and interpretation

A direct validation of data collected in avalanche release areas is usually not possible. It is therefore important to assess the probable accuracy and precision of the sensor system that is used in the area of interest. If the sensor system is prone to systematic errors/inaccuracies, like the DJI Zenmuse L1, it is recommended to use the same equipment and the same flight and survey parameters on all flights. In this way, the influence of systematic errors on change calculations is minimized.

Because avalanche hazards are often accompanied by poor weather conditions (wind, precipitation, low visibility), data collection in unfavorable conditions is inevitable. As a result, data quality will often be compromised. The main challenges related to weather experienced in this project, using the DJI M300 RTK aircraft and the DJI Zenmuse L1 LiDAR scanner, are summarized in Table 6.

**Table 6. Effect of weather conditions on operations and point cloud quality.**

Condition	Possible consequences
High air humidity	Reduced ground point density due to the absorption of light by water molecules.
High air humidity and cold temperatures	In addition to the above, risk of sudden icing on propellers.
Snow	Noise and reduced ground point density due to the reflection of light by snow crystals in the air.

The use of cross-slope flight strips in steep terrain can also affect point cloud quality. As the accuracy decreases with the travel distance of the light pulse, areas covered by both upslope and downslope pulses often suffer from poor strip alignment. Along-slope flight strips should be considered if battery capacity is not a critical factor, especially if the LiDAR sensor used can be directed normal to the terrain.

Ideally, all sources of error and uncertainty are investigated and described before data is published. When fast processing is required, however, the output will be subject to errors that need to be recognized and assessed when interpreting the data. Hence, end users need to be well informed about the potential errors and artifacts associated with each product.

## 4. Conclusions

Extensive testing of UAV remote sensing techniques for snow surface mapping has been carried out in the GEOSFAIR project. This report summarized the findings to optimize survey planning, flight operation and data processing of RGB camera data for photogrammetry and of LiDAR data. It gathers details on implementation of open-source tools (hardware and software) and commercial tools for both flight planning and data processing.

## Appendices

### A Examples of simulated surveys

This appendix details simulated surveys in Storlidalen. The tests are run in a simulated environment to determine the feasibility of flights. Figure A1 shows the estimated elevation flight path for the first mission above Storhaugen avalanche starting area. Figures A2-A5 show post simulation analysis of flights with terrain following at 30 and 50 m terrain spacing. Terrain grid spacing is a setting to the autopilot that controls the grid which is used for requests for terrain data from the aircraft to the ground station. The lower the grid spacing, the closer the aircraft will follow the terrain below.

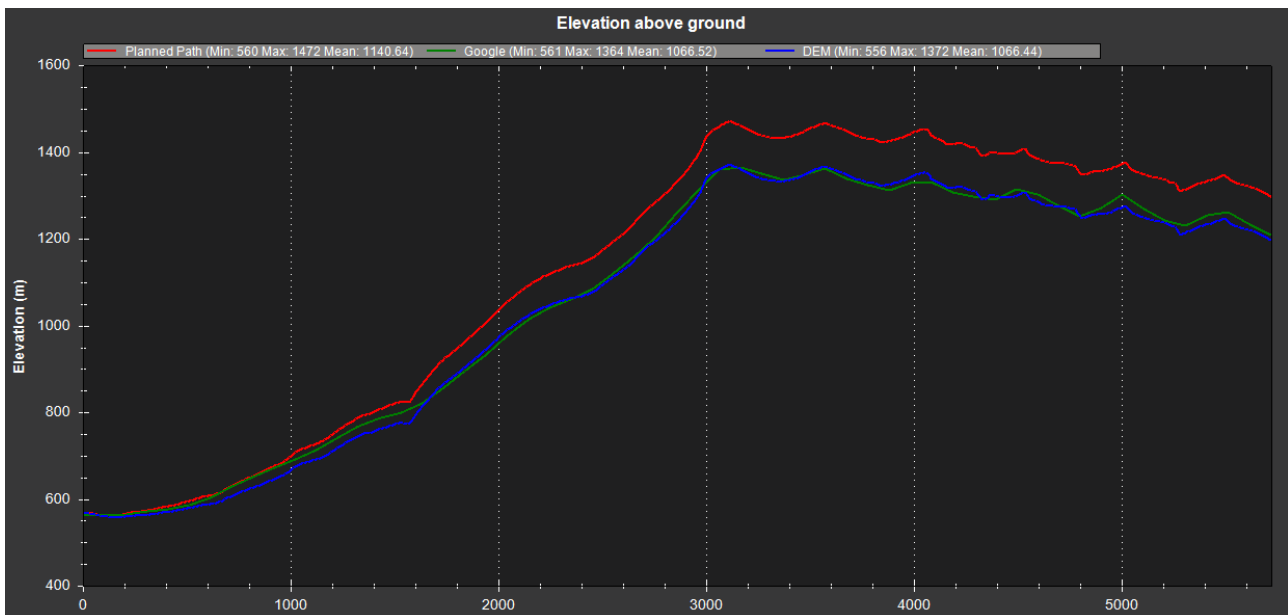


**Figure A1. Planned altitude path (red line) with respect to Google elevation map (green line) versus imported DEM10 (from Norwegian airborne LiDAR, blue line).**

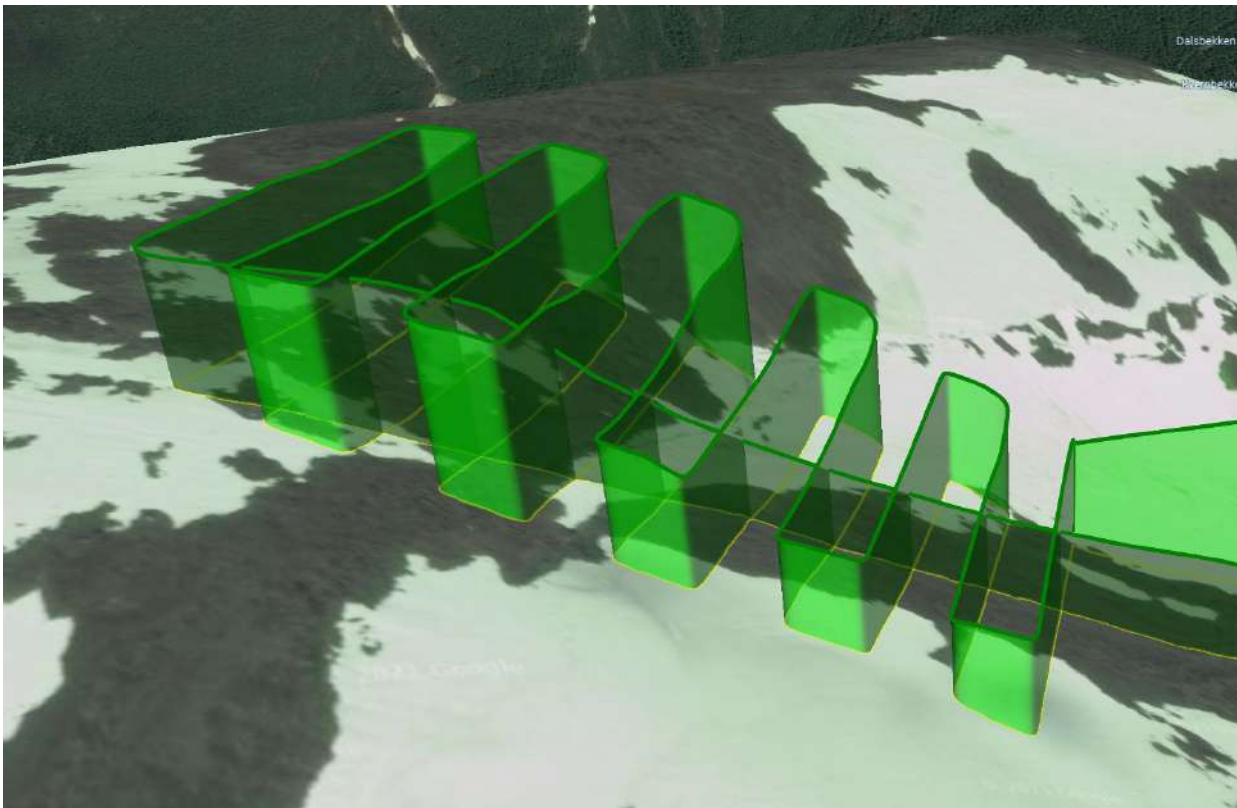


Figure A2. Simulated flight path at 30 m terrain spacing (green line) using DEM10 as terrain following model.

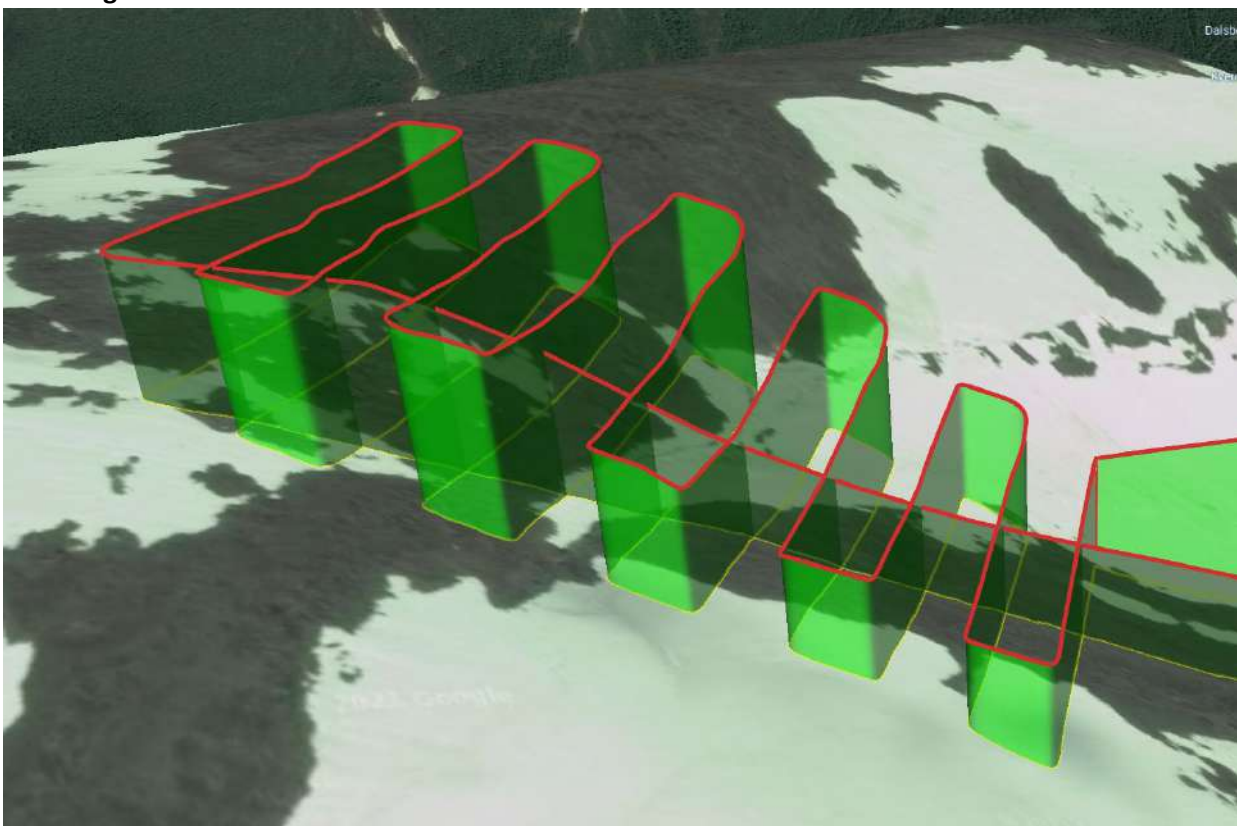


Figure A3. Simulated flight path at 50 m terrain spacing (red line) using DEM10 as terrain following model.

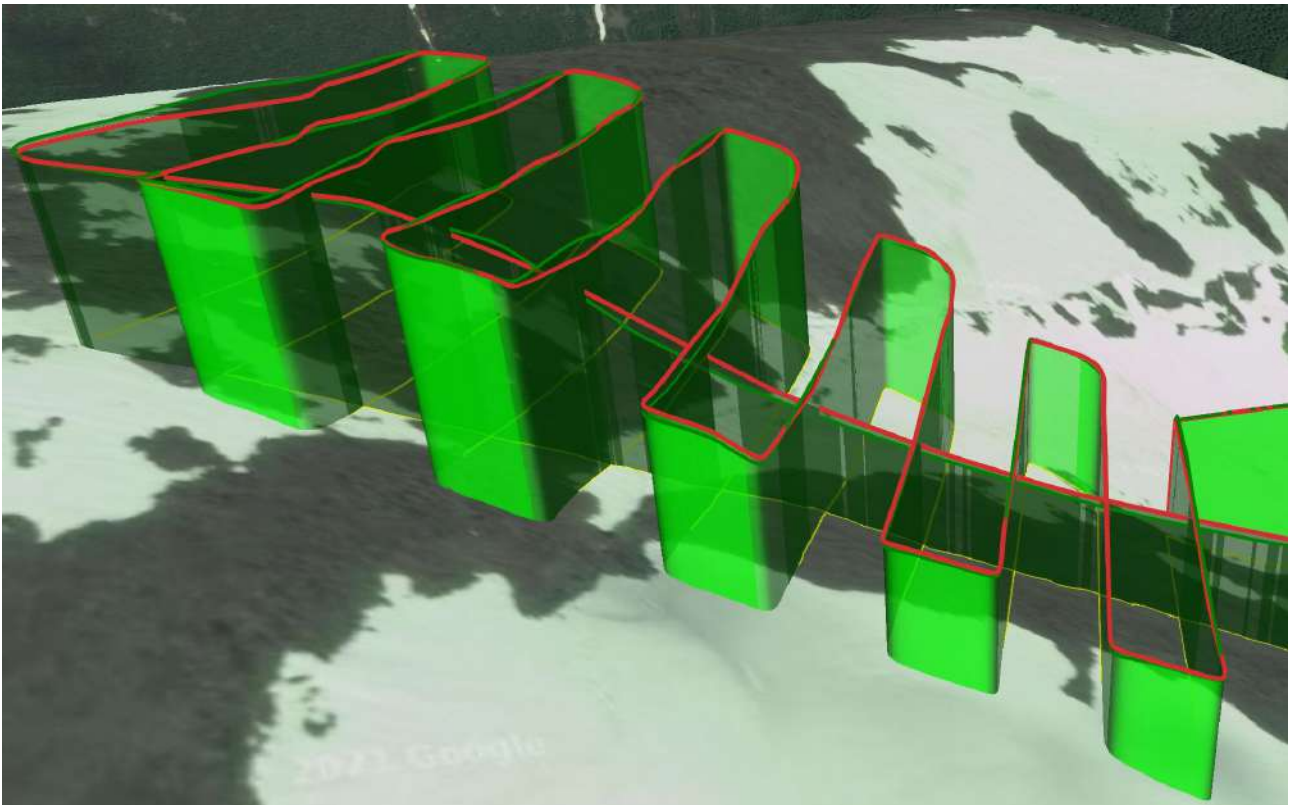


Figure A4. Simulated flight path at 50 m terrain spacing (red line) using DEM10 as terrain following model.

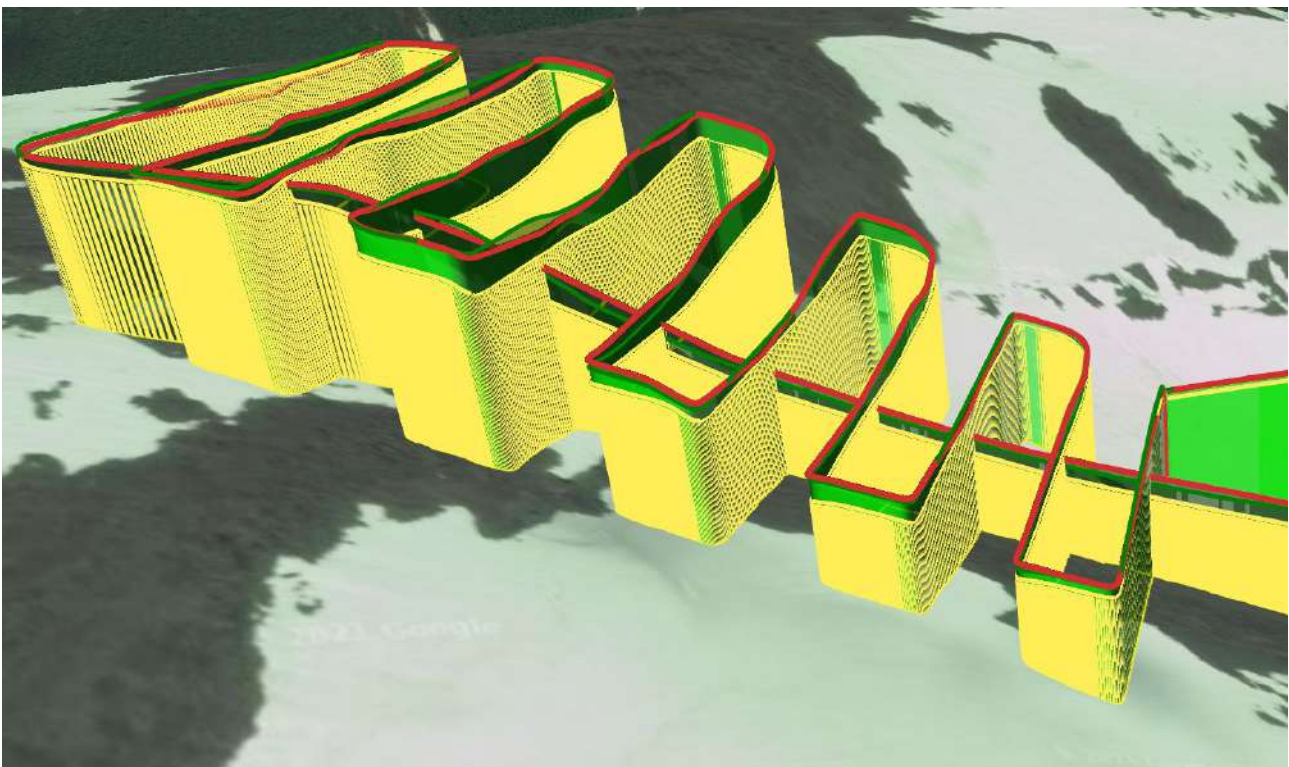


Figure A5. Simulated flight path at 30 (green line), 50 (red line), and 100 m (yellow line) terrain spacing using DEM10 as terrain following model.

Another test of flight plans in Storlidalen valley where the avalanche starting zone is mapped with photogrammetry is displayed in Figure A6. Along the south side of Okla, the simulated results are shown for with 50 and 100 m terrain spacing based on DEM10 model (Figure A7).

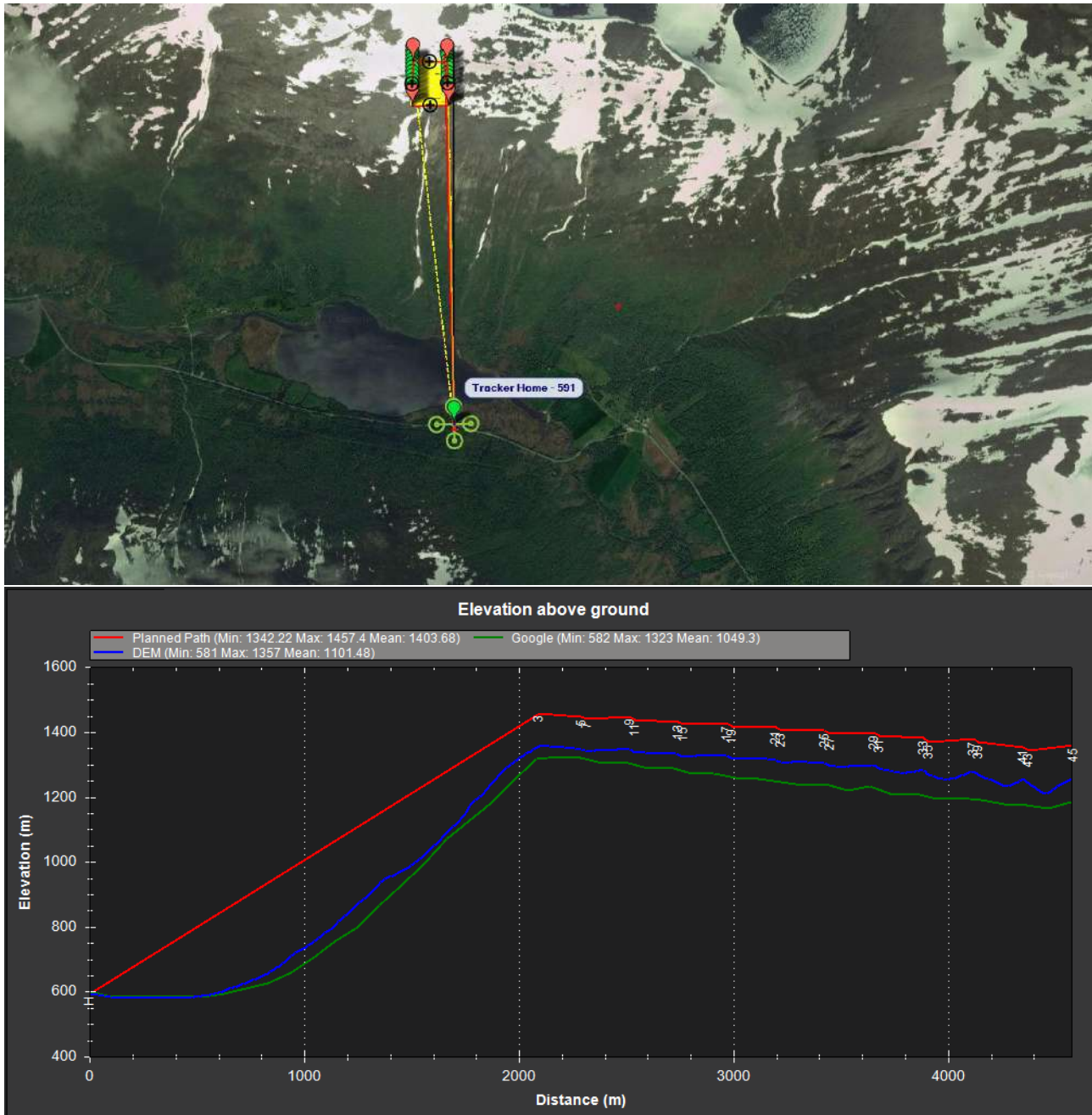


Figure A6. Top: full survey plan to Okla south couloir, with photogrammetry mapping of the top part of the avalanche starting zone. Bottom: planned path (red line) with Google elevation map (green line) versus imported DEM10 (from Norwegian airborne LiDAR, blue line).



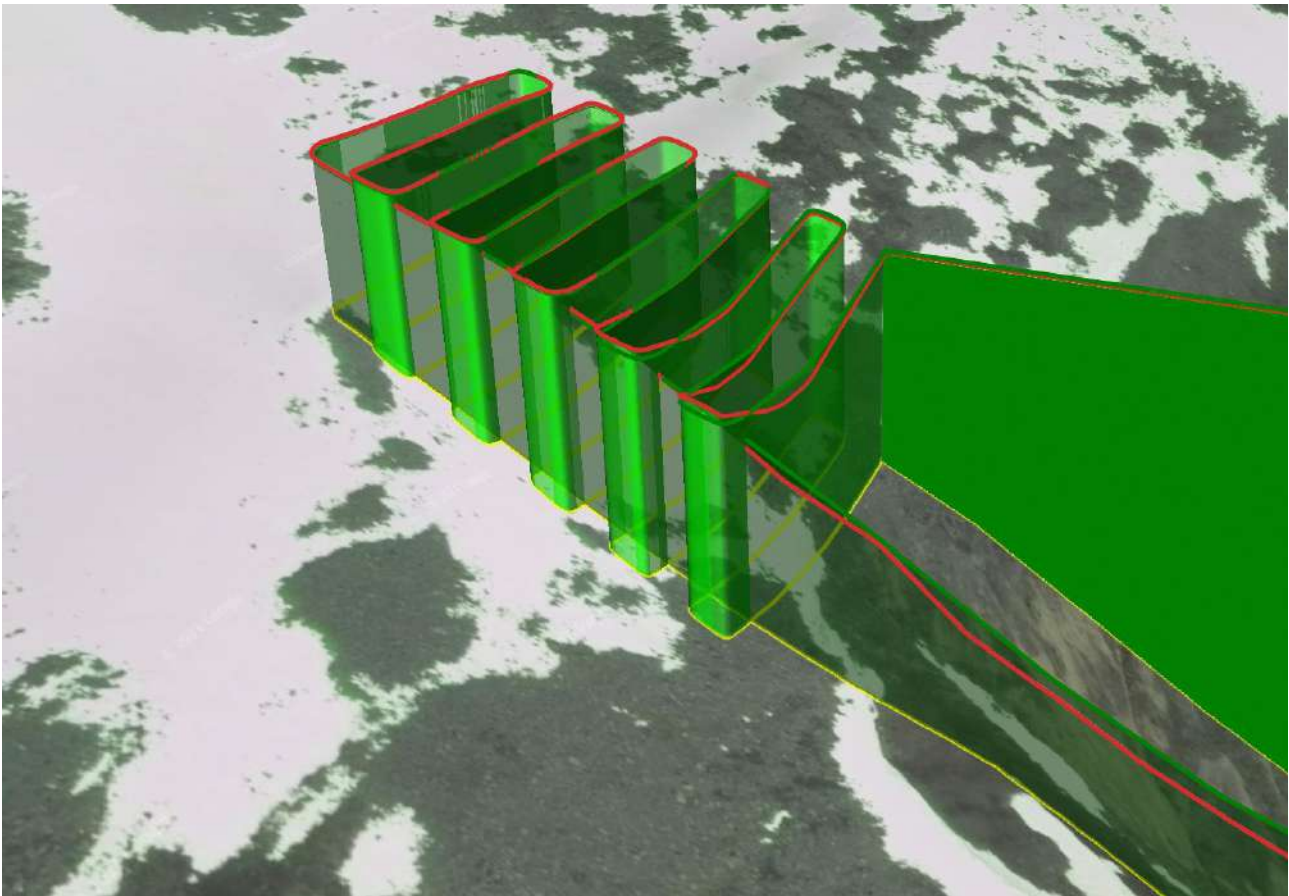


Figure A7. Simulated flight path at 50 m (red line), and 100m (green line) terrain spacing using DEM10 as terrain following model.

## B Examples of processing photogrammetry image sets

Displayed herein are processed images of successful UAV flights that have been obtained from the NPRA. The demonstration shows how a set of missions with geotagged images are processed from a client node containing an SD-card. Upon start, a text file (Figure B1) is created showing a list of paths to the storage device folders, which are then sequentially uploaded to the cloud server for processing. This allows for multiple surveys to be processed in a sequence with no human interference. All sets were processed sequentially in a batch operation with pre-set initial conditions based on the results requirements.

```

1  D:\statens_vegvesen\Bispefonna\2021\20042021
2  D:\statens_vegvesen\Bispefonna\2021\27052021
3  D:\statens_vegvesen\Bispefonna\2021\30042021\Bilder
4  D:\statens_vegvesen\Bispefonna\2021\27052021
5  D:\statens_vegvesen\Fv63Stavbrekkfonna\100_0348
6  D:\statens_vegvesen\Fv63Stavbrekkfonna\100_0349
7  D:\statens_vegvesen\Fv63Stavbrekkfonna\100_0351
8  D:\statens_vegvesen\Fv63Stavbrekkfonna\100_0352
9  D:\statens_vegvesen\Fv63Stavbrekkfonna\100_0353
10 D:\statens_vegvesen\Fv63Stavbrekkfonna\100_0355
11 D:\statens_vegvesen\M300_Breiddalen1_gsd2_o80_s70
12 D:\statens_vegvesen\P4_Grasdalen1_gsd2_o80_s70
13 D:\statens_vegvesen\Trollstigen\02_Bilder_2015
  
```

**Figure B1.** Input text file with the list of surveys to complete as one processing job.

Orthophotos are shown after running through the processing software. All sets were run in batch mode, and uploaded from the client SD card. The results include DEMs and point clouds, which are not shown here, whereas orthophotos are shown as a summary. Total processing time for the 13 sets was in the hours-timeframe, but it depends on resolution requirements and available computer resources. Figure B2 shows a summary of orthophotos from Trollstigen, Breiddalen and Grasdalen. Figure B3 shows processed images from Bispefonna, whereas Figures B4 and B5 show results from Stavbrekkfonna and Storlidalen, respectively.



svv\_Trollstigen\_02\_Bilder\_2015\_01\_13 AGSD 7.2 cm

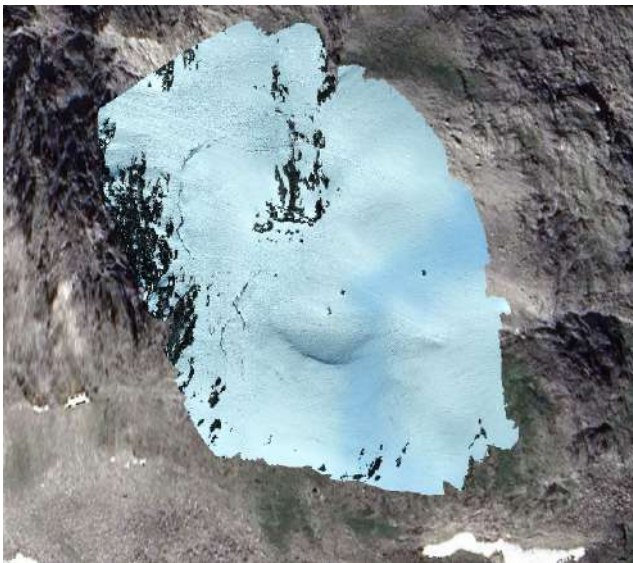


statens\_vegvesen\_M300\_Breiddalen1\_gsd2\_o80\_s70  
03\_08 AGSD 7.2 cm

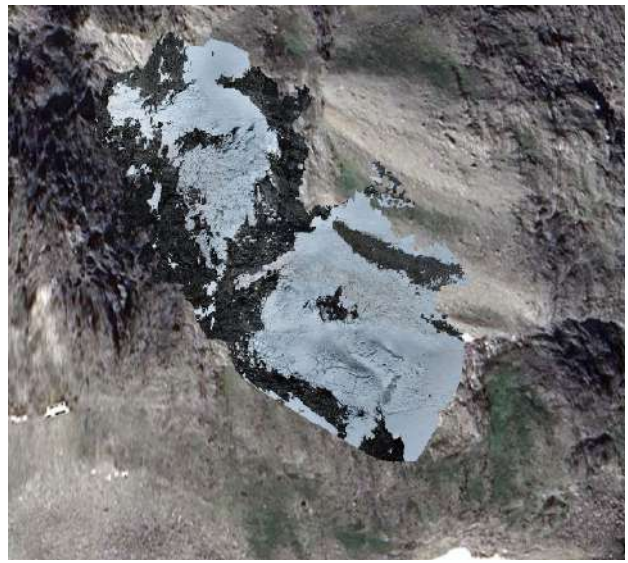


statens\_vegvesen\_P4\_Grasdalen1\_gsd2\_o80\_s70

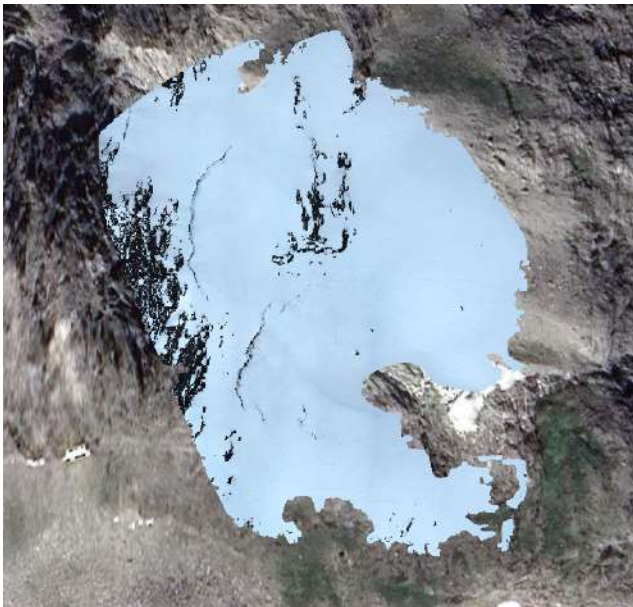
**Figure B2. Orthophotos from Trollstigen (top left), Breiddalen (top right) and Grasdalen (bottom left). Image set provided by NPRA.**



svv\_Bispefonna\_2021\_03\_08



svv\_Bispefonna\_2021\_20042021



svv\_Bispefonna\_2021\_3004



svv\_Bispefonna\_2021\_2705

**Figure B3. Orthophotos from Bispefonna at different time steps during spring melting. Image set provided by NPRA.**



svv\_Fv63Stavbrekkfonna\_100\_0348 AGSD 5.99 cm



svv\_Fv63Stavbrekkfonna\_100\_034 AGSD 5.82 cm



svv\_Fv63Stavbrekkfonna\_100\_0351 AGSD 5.51 cm



svv\_Fv63Stavbrekkfonna\_100\_0352 AGSD 5.24 cm



svv\_Fv63Stavbrekkfonna\_100\_0353 AGSD 5.28 cm



svv\_Fv63Stavbrekkfonna\_100\_0355 AGSD 5.2 cm


**Figure B4. Orthophotos from Stavbrekkfonna at different time steps. Image set provided by NPRA.**

**Signature:**   
Madeline Lee (Jul 9, 2024 00:08 EDT)

**Email:** madeline.lee@sintef.no

**Signature:**   
Peder Eliasson (Jul 9, 2024 22:30 GMT+2)

**Email:** peder.eliasson@sintef.no

**Signature:** 

**Email:** bastien.dupuy@sintef.no



Statens vegvesen  
Pb. 1010 Nordre Ål  
2605 Lillehammer

Tlf: (+47) 22 07 30 00

[firmapost@vegvesen.no](mailto:firmapost@vegvesen.no)

ISSN: 1893-1162

[vegvesen.no](http://vegvesen.no)

**Tryggere, enklere og grønnere reisehverdag**